Excited States in DNA Strands Investigated by Ultrafast Laser Spectroscopy

ARTICLE *in* TOPICS IN CURRENT CHEMISTRY · OCTOBER 2014

Impact Factor: 4.46 · DOI: 10.1007/128_2014_570

3 AUTHORS, INCLUDING:

Yuyuan Zhang
Montana State University
15 PUBLICATIONS **185** CITATIONS

SEE PROFILE

Bern Kohler
Montana State University
109 PUBLICATIONS **4,774** CITATIONS

SEE PROFILE

Top Curr Chem (2014)
DOI: 10.1007/128_2014_570

Excited States in DNA Strands Investigated by Ultrafast Laser Spectroscopy

Jinquan Chen, Yuyuan Zhang, and Bern Kohler

Abstract Ultrafast laser experiments on carefully selected DNA model compounds probe the effects of base stacking, base pairing, and structural disorder on excited electronic states formed by UV absorption in single and double DNA strands. Direct π-orbital overlap between two stacked bases in a dinucleotide or in a longer single strand creates new excited states that decay orders of magnitude more slowly than the generally subpicosecond excited states of monomeric bases. Half or more of all excited states in single strands decay in this manner. Ultrafast mid-IR transient absorption experiments reveal that the long-lived excited states in a number of model compounds are charge transfer states formed by interbase electron transfer, which subsequently decay by charge recombination. The lifetimes of the charge transfer states are surprisingly independent of how the stacked bases are oriented, but disruption of π-stacking, either by elevating temperature or by adding a denaturing co-solvent, completely eliminates this decay channel. Time-resolved emission measurements support the conclusion that these states are populated very rapidly from initial excitons. These experiments also reveal the existence of populations of emissive excited states that decay on the nanosecond time scale. The quantum yield of these states is very small for UVB/UVC excitation, but increases at UVA wavelengths. In double strands, hydrogen bonding between bases perturbs, but does not quench, the long-lived excited states. Kinetic isotope effects on the excited-state dynamics suggest that intrastrand electron transfer may couple to interstrand proton transfer. By revealing how structure and non-covalent

J. Chen
Department of Chemistry and Biochemistry, Montana State University, Bozeman, MT 59717, USA

Department of Chemistry, Emory University, Atlanta, GA 30322, USA

Y. Zhang and B. Kohler (✉)
Department of Chemistry and Biochemistry, Montana State University, Bozeman, MT 59717, USA
e-mail: kohler@chemistry.montana.edu

interactions affect excited-state dynamics, on-going experimental and theoretical studies of excited states in DNA strands can advance understanding of fundamental photophysics in other nanoscale systems.

Keywords Base pairing · Base stacking · Charge transfer state · DNA photophysics · Excimer · Excited-state dynamics · Exciton · Femtosecond transient absorption · Proton-coupled electron transfer

Contents

1 Introduction
2 Ultrafast Spectroscopy Techniques
3 Nucleic Acid Structure
  3.1 Base Stacking
  3.2 Base Pairing
  3.3 Structural Complexity and Disorder
  3.4 Electronic Structure
4 Excited-State Dynamics in Single Strands
  4.1 Dinucleotides
  4.2 Single-Stranded Oligonucleotides
5 Excited-State Dynamics in Base Pairs and in Double-Stranded DNA
  5.1 Single Base Pairs
  5.2 Double-Stranded Oligonucleotides
6 Summary and Outlook
References

Abbreviations

2AP	2-Aminopurine
8-oxo-dGuo	8-Oxo-7,8-dihydro-2′-deoxyguanosine
A	Adenine
AMP	Adenosine 5′-monophosphate
ATP	Adenosine 5′-triphosphate
C	Cytosine
CASPT2	Complete active space with second-order perturbation theory
CD	Circular dichroism
CI	Conical intersection
CPD	Cyclobutane pyrimidine dimer
CR	Charge recombination
CT	Charge transfer
dAMP	2′-Deoxyadenosine 5′-monophosphate
DFT	Density functional theory
ECCD	Exciton-coupled circular dichroism
ESA	Excited-state absorption

ESPT	Excited-state proton transfer
ET	Electron transfer
FC	Franck–Condon
FTIR	Fourier-transformed infrared spectroscopy
FU	Fluorescence upconversion
G	Guanine
GSB	Ground-state bleaching
IC	Internal conversion
IET	Intermolecular energy transfer
KIE	Kinetic isotope effect
MCT	Mercury-cadmium-telluride
O	8-Oxo-7,8-dihydro-2′-deoxyguanosine (in a DNA sequence)
PCET	Proton-coupled electron transfer
PMT	Photomultiplier tube
PT	Proton transfer
QM/MM	Quantum mechanical/molecular mechanical
RI-ADC(2)	Algebraic diagrammatic construction to second-order with resolution of the identity
T	Thymine
TA	Transient absorption
TCSPC	Time-correlated single photon counting
TD-DFT	Time-dependent density functional theory
TRIR	Time-resolved infrared spectroscopy
U	Uracil
UV	Ultraviolet
VC	Vibrational cooling
VUV	Vacuum ultraviolet
WC	Watson–Crick

1 Introduction

Photodamage to the genome is initiated by excited electronic states formed in DNA by the absorption of UV photons. Although the intensity of solar UV radiation reaching the surface of earth is attenuated by stratospheric ozone, excitation of DNA is highly efficient on account of the strong $\pi^* \leftarrow \pi$ transitions of the nucleobases: adenine (A), guanine (G), cytosine (C), thymine (T), and uracil (U). In order to *minimize* photochemical damage and *maximize* the photostability of the genome, DNA excited states should decay to the electronic ground state rapidly and with high quantum efficiency. Low fluorescence quantum yields and low photoproduct quantum yields provide evidence that this is the case, but detailed understanding of the rapid nonradiative decay pathways which deactivate excited states has been the goal of many investigators during the past decade.

The excited states of the naturally occurring nucleobase monomers have been studied intensively and there is growing consensus about photophysical decay channels [1, 2]. As the understanding of excited states of single nucleobases has grown, the complex photophysics in base multimers has attracted increased attention. The trend toward studying more complex systems has been aided on the one hand by better understanding of the excited states of single bases – the building blocks of DNA and RNA strands – and on the other by advances in computing power and quantum chemical methods which enable increasingly sophisticated calculations of the electronic structure of multi-base systems. Whereas calculations of excited states of single bases were considered to be barely tractable in 2000, high-level ab initio calculations are now performed on systems containing multiple bases.

Singlet excited states of nucleobase monomers decay in hundreds of femtoseconds to the electronic ground state. Typically, a nearly barrierless pathway leads from the Franck–Condon (FC) region to S_1/S_0 conical intersections (CIs) which cause the UV-excited nucleobases to return nonradiatively to their ground states on a time scale of hundreds of femtoseconds [1–5]. Other chapters in this volume provide detailed accounts of the nonradiative decay pathways of single bases in solution and in the gas phase, but we begin with this brief generalization about the ultrashort lifetimes of single nucleobases in order to highlight the unexpectedly long lifetimes seen in DNA strands. Excited states lasting tens to hundreds of picosecond are commonplace in single- and double-stranded DNA/RNA [1, 4, 6]. Current evidence suggests that the environment in a DNA strand doesn't just prolong the lifetime of excited states localized on single bases, but instead creates new classes of excitations and new photophysical pathways not found in base monomers. A full understanding of these mechanisms is not yet available, but this chapter will emphasize growing evidence that the relevant couplings act at short distances and are the result of π–π stacking between nucleobases.

A theme of this chapter is the link between structure and excited-state dynamics. This connection reveals why interest in DNA excited states goes beyond their pertinence to photodamage. First, the non-covalent interactions which give DNA its structure are the same as those found in other supramolecular and nanoscale architectures made from smaller organic building blocks. Consequently, knowledge of how these interactions mediate energy and electron transfer (ET) in DNA may provide a better understanding of these fundamental events in other systems. Second, excited states in DNA are strongly influenced by structure, and they can thus serve as powerful probes of dynamical motions in a DNA molecule. During the short lifetimes of excited states of native bases, large-amplitude motions such as backbone torsions or rotations about glycosidic bonds are limited, and the shortest-lived excited states probe static structures, as in the case of thymine dimer photochemistry [7, 8]. A significant fraction of excited states formed in base stacks have lifetimes of up to several hundred ps [9], making them sensitive to conformational fluctuations on longer time scales. Finally, modified bases such as 2-aminopurine (2AP) have lifetimes in the nanosecond range, as monomers [10–12], and can potentially probe dynamics on still longer time scales. Comprehensive knowledge

of decay pathways of excited states of native and modified nucleobases, and of other excited state probes, is critical for extracting insights into the structural dynamics of nucleic acids from time-resolved spectroscopy.

This chapter reviews current understanding of excited states in single- and double-stranded DNA in aqueous solution obtained from ultrafast laser experiments. Although many of the model systems of greatest interest to us have been studied only by the femtosecond transient absorption (fs-TA) technique, results from time-resolved emission techniques, such as time-correlated single photon counting (TCSPC) and femtosecond fluorescence upconversion (fs-FU), will be discussed when appropriate. Comparison of results obtained from time-resolved absorption and emission experiments can bring greater insights than is possible from either technique alone. The femtosecond laser techniques used to observe excited-state dynamics in DNA model compounds are outlined in Sect. 2. The transient absorption and time-resolved emission techniques are discussed briefly with emphasis on what these techniques reveal about excited-state dynamics in DNA strands.

Section 3 discusses the three-dimensional structures adopted by the nucleic acid model compounds which have been most studied to date, including dinucleotides, and single- and double-stranded oligonucleotides. The spatial arrangement of nucleobases in DNA determines the couplings that give rise to new deactivation pathways not found in base monomers. The underlying interactions responsible for nucleic acid structure are also discussed. These are sufficiently weak that it is more accurate to consider the distribution of structures present in solution at ambient temperature than to imagine a single, well-defined structure. The relatively flat free energy landscapes governing the three-dimensional structure of nucleic acids are responsible for the structural disorder which must be carefully considered in order to interpret experimental results correctly. This section ends with an overview of excited states created by UV radiation in DNA strands.

Section 4 begins by summarizing experimental evidence that π–π stacking by nucleobases gives rise to fundamentally new decay channels. These effects are already seen in minimal π stacks of just two bases, so our discussion begins with the time-resolved spectroscopy of dinucleotides before taking up excited states in longer single strands containing more than two bases. The effects of base pairing on excited states are discussed in Sect. 5 for single base pairs in solution and for larger systems in which bases are both stacked and paired. The progression from dinucleotides to duplex DNA emphasizes how excited states in simpler model systems are influenced by the increasing complexity found in larger ones. Finally, Sect. 6 presents a summary and an outlook describing unsolved issues and promising new research directions.

2 Ultrafast Spectroscopy Techniques

The lifetimes of excited states of DNA strands are often orders of magnitude longer than those of single bases [13], as discussed in Sects. 4 and 5. These observations from time-domain spectroscopy have been a driving force for advancing understanding of DNA photophysics. Indeed, the ability to observe excited-state dynamics of DNA directly in the time domain with femtosecond time resolution has been singularly important to progress in the field. The well-known fact that the steady-state absorption spectrum of a DNA strand is very similar in appearance to the sum of the spectra of its constituent nucleotides points out the limits of relying solely on frequency-domain spectroscopy to understand excited states of DNA strands in solution.

In this section, we review the ultrafast spectroscopic techniques used to study excited-state dynamics in DNA with an emphasis on the observables and the inferences that can be obtained from them. The aim is to provide non-specialists and beginning researchers with an overview of the ultrafast laser techniques used to study DNA excited states with just enough detail so that the conclusions that practitioners of these techniques have drawn from their experiments can be better understood. Readers interested in technical details of any of the techniques may consult the cited references for more information.

Because our focus is on solution studies, we will exclude the many innovative techniques used to study DNA model compounds in the gas phase. An overview of gas-phase spectroscopic techniques is provided in Sect. 3 of [5], and descriptions of femtosecond pump-probe experiments that use sensitive photoionization detection of electrons and molecular ions to compensate for the low number densities of gas-phase species provide additional details [14–16].

Ultrafast laser techniques for studying excited states of DNA in solution can be divided into techniques that monitor absorption or techniques that monitor emission as a function of time after the sample is excited by an ultrashort (femtosecond or picosecond) laser pulse. Because nucleic acids made from the canonical bases absorb only very weakly above 300 nm, most spectroscopic studies have used UVB or UVC laser pulses, although more concentrated solutions of oligonucleotides have recently been studied using UVA excitation [17]. The third harmonic output from a titanium sapphire laser system – the nearly universal source used in femtosecond experiments – is conveniently located near 260 nm, in the vicinity of the wavelength of maximum absorption of most DNA samples. Tunable deep UV pulses can be generated from the ~800-nm fundamental using various frequency upconversion schemes and optical parametric amplification. Many modified bases [10, 11] absorb at longer wavelengths (>300 nm) than the canonical bases, making it possible to excite these chromophores selectively when they are incorporated in a DNA strand.

In the femtosecond transient absorption (fs-TA) technique, a femtosecond pump pulse creates initial excited states (thick purple arrow in Fig. 1a), which are detected through changes in the transmission of a time-delayed probe pulse (Fig. 1a–e).

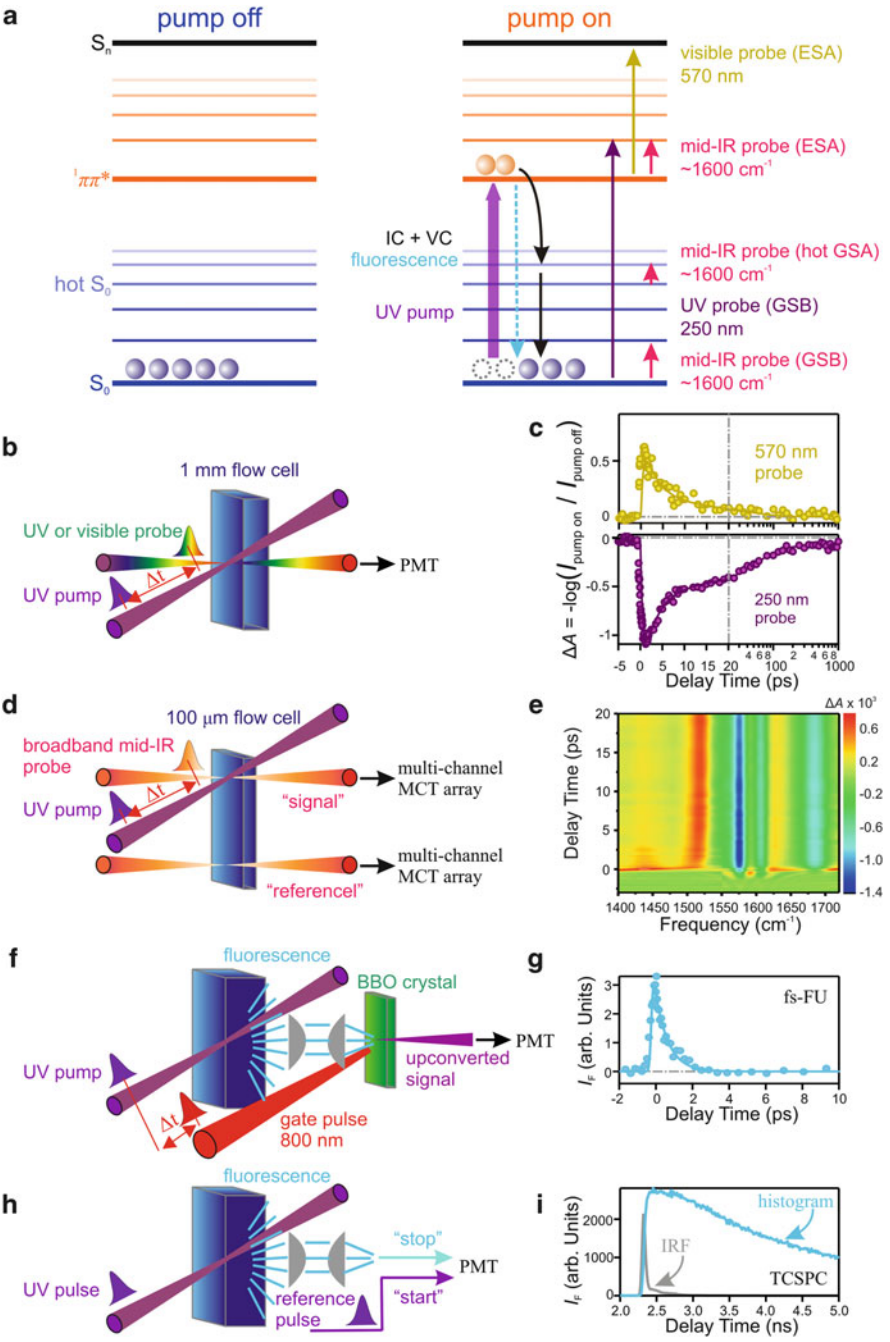

Fig. 1 (**a**) Ground- and excited-state populations in a DNA model compound before (*left*) and after (*right*) excitation by a UV pump pulse to a $^1\pi\pi^*$ state (*thick purple arrow*). After photoexcitation, the excited-state population returns to the ground state via fluorescence (*blue dashed arrow*), or ultrafast internal conversion followed by vibrational cooling (IC + VC, *black arrows*). Decay to charge transfer/excimer or other excited states is also possible, but not shown.

Many fs-TA experiments on DNA systems use UV- (long thin purple arrow in Fig. 1a) and visible-wavelength probe pulses (thin gold arrow in Fig. 1a), which monitor electronic transitions, but mid-IR probe pulses (red arrows in Fig. 1a) obtained by difference-frequency mixing of two near-IR pulses provide an alternative way to study excited states through measurement of time-dependent vibrational resonances in both ground and excited electronic states. The TA technique with mid-IR probe pulses is often referred to as time-resolved IR (TRIR) spectroscopy [18, 19]. Schematic illustrations of these TA techniques and typical signals are shown in Fig. 1b–e. Additional experimental details about these techniques can be found in the literature [18, 20–22].

In all fs-TA experiments, excited states created by the excitation or pump pulse, as well as any excited states or photoproducts populated at later times, are detected through changes in the transmission of the probe pulse. The TA signal, whether measured at a single wavelength or in broadband mode, records changes in the sample absorbance (ΔA) induced by the pump pulse and calculated as

$$\Delta A = -\log\left(\frac{I_{\text{pump on}}}{I_{\text{pump off}}}\right), \tag{1}$$

where $I_{\text{pump on}}$ and $I_{\text{pump off}}$ are the probe pulse intensities measured at the detector with and without the presence of the pump pulse, respectively. The probe beam can be split into "signal" and "reference" portions – the former is spatially overlapped with the pump pulse, while the latter is not – in order to reduce the shot-to-shot noise and improve the instrument sensitivity (Fig. 1d). In this case, ΔA is calculated using (2):

$$\Delta A = -\log\left(\frac{I_{\text{signal, pump on}} \,/\, I_{\text{reference, pump on}}}{I_{\text{signal, pump off}} \,/\, I_{\text{reference, pump off}}}\right). \tag{2}$$

TA is therefore a form of difference spectroscopy. The contribution to the TA signal from each transient species is proportional to its population multiplied by the difference between its absorption cross section and the cross section of the ground

Fig. 1 (continued) The excited-state population can be probed by visible (*gold arrow*) or mid-IR (*top red arrow*) pulses. UV (*deep purple arrow*) or mid-IR (*bottom red arrow*) pulses can be used to monitor the ground state population. Mid-IR can also probe the hot ground state absorption (*middle red arrow*). (**b–i**) Schematic illustrations of various ultrafast laser methods and representative signals. (**b**) fs-TA experiment using a single-color UV or visible probe pulse and (**c**) typical kinetic traces produced by visible probe-detected ESA (*top*) and UV-probe GSB (*bottom*). (**d**) fs-TRIR with broadband mid-IR probing showing the use of a reference beam to improve the signal-to-noise ratio. Signal and reference beams are spectrally dispersed in a spectrograph and detected by dual multi-element Mercury-Cadmium-Telluride (MCT) arrays cooled by liquid nitrogen. (**e**) Representative time- and frequency-resolved fs-TRIR data. (**f**) fs-FU technique and (**g**) a typical emission transient. (**h**) TCSPC experiment and (**i**) typical data. Note the 1,000-fold difference in time scale in (**g**) and (**i**)

state from which the transient population originated with both cross sections measured *at the probe wavelength*.

Exited-state absorption (ESA), ground-state bleaching (GSB), and stimulated emission can all contribute to TA signals. The importance of each depends on the probe wavelength chosen and the cross sections for the relevant transitions. ESA by the lowest $^1\pi\pi^*$ states of the base monomers gives rise to broad and featureless bands at visible and near UV wavelengths. For the canonical bases, a broad band occurs with λ_{max} near 600 nm, and a second, stronger, band is observed with λ_{max} below 400 nm [23, 24].

The decay of ESA at visible probe wavelengths was used to make the first accurate measurements of the $^1\pi\pi^*$ state lifetimes of DNA and RNA nucleosides in 2000 [25, 26]. The ESA cross sections of the lowest singlet excited states (S_1 states) of the various bases are very weak, and care should be taken to differentiate these signals from absorption by solvated electrons, which are easily produced by the high intensity pump pulses used in femtosecond laser experiments [26]. The detailed procedure used in our laboratory for subtracting the solvated electron signals is described in [27]. The weak ESA signals make TA studies with broadband detection difficult, and detailed comparisons of ESA spectra for the various base monomers are unavailable. Nonetheless, current information suggests that ESA spectra of the $\pi\pi^*$ singlet states of the base monomers are very similar. For example, the broadband TA spectra are remarkably similar for adenine and guanine [23, 24]. This lack of differentiation is perhaps unsurprising, given their similar ground-state absorption spectra. Too little is known about ESA spectra of base multimers to offer generalizations.

A powerful alternative to measuring excited-state lifetimes is to interrogate the repopulation of the ground state in GSB recovery experiments. In these measurements, the probe wavelength in an fs-TA experiment is tuned to a region where the ground state molecules absorb, typically in the deep UV (e.g., 250 nm) for nucleobases (thin purple arrow in Fig. 1a). The GSB signals can easily be measured because of the large ground-state absorption cross sections of the nucleobases, and GSB signals can be readily interpreted because interference from solvated electrons, which absorb negligibly at UV wavelengths [28], is greatly reduced. The obtained ΔA signal is negative, signifying the removal of ground-state population by the UV pump pulse (see (1) and (2)). As excited molecules return to the ground state, the ΔA signal approaches zero (purple trace in Fig. 1c). The observed kinetics thus measures the time for population to return to the thermally equilibrated electronic ground state. Significantly, this time can be measured without knowledge of the series of states that excited molecules pass through. Particularly when a small number of excited states or intermediates are involved, bleach-recovery TA measurements can make it possible to observe clearly the dynamics of excited states that may have weak excited-state absorption, or which may absorb at unknown wavelengths, and therefore be difficult to study. For example, bleach recovery measurements first identified a longer-lived excited state in pyrimidine nucleobases [29].

A critically important point is that whenever the time to jump from an excited state to the ground state in a nonradiative transition is short compared to the time required for solute-solvent vibrational energy transfer, the GSB kinetics are dominated by decay of vibrationally hot ground state molecules. In this case, the GSB signals measure the time for vibrational cooling (VC) and not the faster time that corresponds to the initial transition to the ground state. The ultrashort lifetimes of monomeric bases thus cause GSB signals to decay up to an order of magnitude more slowly than the disappearance of ESA at visible wavelengths. Because of its hydrogen-bonding network, VC proceeds with remarkable speed in water. Ultrafast internal conversion (IC) produces ground state molecules with an initial vibrational temperature on the order of 1,000 K. Nonetheless, this excess vibrational energy is transmitted to the solvent with a time constant of just 2 ps for adenine [30], while somewhat slower times of 5 or 6 ps have been observed for nucleobase derivatives such as caffeine which have fewer hydrogen bond donor groups [21]. In fs-TA experiments that monitor GSB kinetics, bleached ground state signals frequently exhibit a several picosecond component, and this is a valuable indicator that at least some excited states in a DNA model compound have returned via IC on a time scale that is faster than VC (i.e., faster than several picoseconds).

In fs-TA experiments, the kinetics observed at very early times, i.e., within the pulse duration of the pump and probe pulses (typically, $t < 200$ fs), are usually contaminated by signals arising from two-photon absorption [31] and/or cross phase modulation [32] from the sample (typically the solvent because of its high concentration) or the cell windows (if a static or flow cell is used). These signals, frequently called "coherent artifacts," are seen when the pump and probe pulses are temporally overlapped, and thus hinder the ability to observe extremely fast kinetics. In order to probe shorter time scales, ultrashort UV pulses produced by four-wave mixing [33] and a windowless, free-flowing liquid jet [34] can be used. Note, however, that the former increases the peak intensity of the pump pulses, while the latter usually requires solution volumes larger than are practical for DNA samples. Importantly, analysis of our fs-TA signals is restricted to delay times longer than ~200 fs to avoid these issues.

Because of inhomogeneous and homogeneous broadening, electronic transitions in DNA model compounds usually overlap strongly, making it difficult to disentangle kinetics from fs-TA experiments. fs-TRIR experiments monitor vibrational resonances (red arrows in Fig. 1a) and have the advantage that overlap between vibrational transitions can be greatly reduced, aiding kinetic interpretation. Typically, each nucleobase has one or more distinctive vibrational bands in the double-bond stretching region, where strong transitions caused by carbonyl and ring stretches are observed. These experiments are typically carried out in D_2O solution because of its greater mid-IR transmission compared to H_2O. As will be discussed below, the localized, base-specific character of vibrational modes offer an exciting, but underutilized approach to investigate excited states in multichromophoric systems.

In fs-TRIR experiments, the broad bandwidth of the mid-IR pulses (~200 cm^{-1} for a 100-fs pulse with a center wavelength of ~6 μm) is used to record ΔA signals

as a function of both time and frequency, producing two-dimensional data as in the example shown in Fig. 1e. As in the case of the fs-TA experiments that probe electronic transitions, fs-TRIR signals are composed of negative and positive signals. Negative signals arise from bleaching of ground-state vibrations, while positive signals arise from vibrations in excited electronic states and from fundamentals of highly vibrationally excited ground-state molecules. The latter species show distinctive sigmoidal signals in which the bleaching of a ground state resonance is accompanied by positive absorption on its red edge caused by anharmonicity [35]. This is the distinctive signature of VC dynamics in fs-TRIR experiments.

When excited states generated by the pump pulse can decay radiatively (blue dashed line in Fig. 1a), time-domain emission measurements are possible. Measurements can be made on ultrafast time scales using the Kerr-gated time-resolved fluorescence technique [23] or, more commonly, by fluorescence upconversion [36]. In the femtosecond fluorescence upconversion (fs-FU) technique, emission from the solution sample is typically collected using a parabolic mirror (illustrated by a lens system in Fig. 1f in order to simplify the illustration) and subsequently mixed with a time-delayed, femtosecond gate pulse in a nonlinear optical crystal to generate an upconverted signal at a higher frequency (Fig. 1f, g). Varying the arrival time of the gate pulse at the mixing crystal allows the emission decay to be recorded with subpicosecond time resolution. Importantly, fluorescence lifetimes obtained by fs-FU experiments on nucleobase monomers [36–39] are in excellent agreement with the decay time of ESA signals measured in fs-TA experiments [25, 26]. However, discrepancies between fs-TA and fs-FU measurements on DNA strands have occasionally led to confusion about excited-state decay pathways. Dynamic range limitations mean that upconversion experiments emphasize emission by brighter $^1\pi\pi^*$ states and it can be difficult to detect emission from darker states.

The extremely sensitive time-correlated single-photon counting (TCSPC) technique can detect smaller populations than can be accurately quantified in either fs-TA or fs-FU experiments. However, this method achieves sensitivity at the cost of time resolution. In TCSPC, no gate pulse is used and emission is measured directly using a fast photodetector and specialized electronics. Typically, time resolution of several tens of picoseconds is achieved using a micro-channel plate photomultiplier tube (PMT) (Fig. 1h, i). Because TCSPC measurements cannot measure the fastest emission decay components, it is necessary to combine them with fs-FU measurements to obtain a complete picture of the emission over many decades in time [40]. Notably, the high sensitivity of the TCSPC method means that the characterization of extremely weakly emitting DNA excited states could be adversely affected by impurities, and careful background correction and well-designed protocols are essential [41].

The time resolution achievable with each of the above techniques is an important experimental consideration. In all pump-probe techniques, varying the path length traversed by one of the pulses using a retroreflector mounted on a computer-controlled translation stage is used to control the delay time between pulses.

The time resolution is independent of the response time of the photodetector used, and is determined instead by the temporal widths of pump and probe pulses, which can be as short as ~10 fs. The group velocity of a femtosecond laser pulse is a function of its center wavelength. For this reason, femtosecond pulses with widely separated center wavelengths transit the solution sample at different speeds. This effect causes initially synchronized pump and probe pulses to "walk off" one another, degrading the time resolution. The walk off problem in fs-TRIR experiments is mitigated somewhat by the thinner sample path length of ~100 μm compared to the 1 mm path length which is typical of fs-TA measurements with visible and UV probe pulses. For the instrumentation in our laboratory, an instrument response function of between 100 and 200 fs is achieved for visible and UV probe experiments, while our fs-TRIR measurements have a time resolution of approximately 400 fs. Geometrical factors can smear the arrival times of emitted photons at the upconversion crystal and the time resolution of our upconversion setup is around 300 fs.

The fs-TA technique requires high intensity pulses with single-pulse energies of hundreds of nanojoules or more. These pulses are provided by a chirp-pulse amplified titanium sapphire laser system. TCSPC and fs-FU measurements do not require high pulse energies and the excitation source can be an unamplified femtosecond oscillator. The typical pulse repetition rate of an unamplified laser system of 80 MHz compared to the kilohertz repetition rate of an amplified source is a key to the high signal-to-noise ratio obtainable with TCSPC instrumentation.

3 Nucleic Acid Structure

The striking differences between excited state relaxation in single bases and in DNA and RNA strands are the result of how the bases are arranged in space. Knowledge of nucleic acid structure is thus a prerequisite for understanding nonradiative decay pathways. The spatial arrangements of the absorbing moieties in multichromophoric molecules such as DNA determine the couplings responsible for decay channels such as energy and electron transfer which are not possible in single chromophores.

The non-covalent interactions of base stacking and base pairing are responsible for DNA secondary structure and thus control the separation between coupled bases and their mutual orientations. However, it must be kept in mind that nucleic acid structures are constantly fluctuating in aqueous solution at physiological temperature – a fact which may be forgotten when one considers only the familiar yet static structures of double helical DNA obtained from X-ray crystallography. Because most nucleic acid model systems do not populate deeply trapped structures, it is vital to consider structural heterogeneity and disorder. Most di- and oligonucleotides are characterized by broad distributions of structures, which may be separated by free energy barriers that are no greater than thermal energy (k_BT). Of course, this heterogeneity fulfills a biological purpose – DNA's marginal stability enables

enzymes and other molecules to interact with, process, and alter DNA at physiological temperatures.

In this section, we emphasize the structural attributes of DNA important for interpreting photophysical experiments and provide an overview of DNA electronic structure. Here, "DNA" is shorthand for all nucleic acid model compounds, including those with RNA backbones, chosen by experimentalists for ultrafast laser experiments. The choice of compounds is driven by a reductionist philosophy and many of the systems (e.g., dinucleotides) are obviously far removed from what a biologist understands by DNA (or RNA). Nevertheless, even these "simple" model systems have considerable structural complexity that must be understood to interpret spectroscopic experiments correctly.

3.1 Base Stacking

The nucleobases are planar aromatic molecules which tend to aggregate (self-associate) in aqueous solution even when they are not covalently linked [42, 43]. This tendency is greatest for the purine bases with their larger hydrophobic surfaces, but it is also significant for the pyrimidines. The nucleobases form stacked dimers that resemble the sandwich geometries adopted by dye molecules that form H-aggregates [44]. The distinguishing feature of a base stack is that both bases lie in parallel or nearly parallel planes and are in van der Waals contact. The perpendicular distance between bases is on the order of ~3.4 Å and solvent molecules are excluded from the region of base-base overlap seen when the stack is viewed along a direction perpendicular to the base planes (Fig. 2).

The π–π stacking or base stacking geometry is a distinctive feature of DNA structure and one that accounts for most of the stabilization energy of the double helix [45]. Bases in single-stranded DNA also stack and this can be detected through both classical methods such as exciton-coupled circular dichroism (ECCD) [46–49] and UV melting (hypochromism) [45], as well as through less well-known techniques such as single-molecule stretching experiments [50, 51], velocity sedimentation analysis [52], and from the electrophoretic mobility of gapped duplexes [53].

In contrast to duplex forms, single strands melt non-cooperatively over a broad temperature range and are not amenable to study by X-ray crystallography. MD simulation can potentially provide insights into both structure and dynamics in atomistic detail, but the popular force fields used in these simulations may overstabilize base-stacked structures [54, 55]. Consequently, there is considerable uncertainty about both the distribution of structures that a single-stranded oligonucleotide can adopt in aqueous solution and the time scales for structural interconversion.

The full specification of the geometry of a stack of two bases requires some of the same coordinates used for stacked base pairs [56]. One of the bases may be

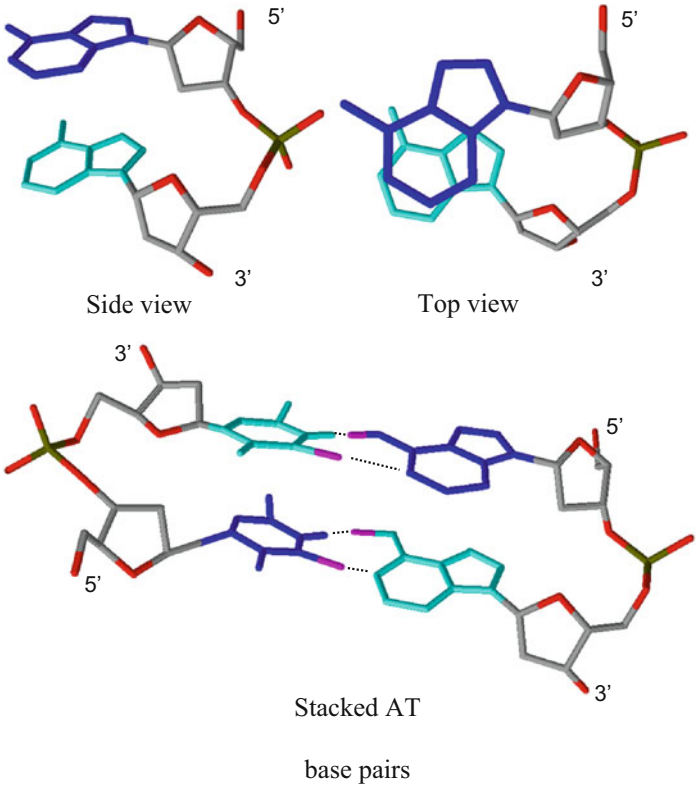

Fig. 2 *Top*: Structure of dApdA showing the face-to-back stacking motif found in the B-DNA helix. The 5′ base is shown in *dark blue*, and the 3′ base is shown in *light blue*. The *top view at right* shows that the bases form a right-handed helix (the 5′ base is on top) and illustrates the region of base-base overlap. *Bottom*: Stacked adenine and thymine base pairs with hydrogen bonds shown by *dashed lines*. Structures are illustrative and were drawn using the ACD/ChemSketch software

displaced in a direction parallel to its base plane (a parameter known as slide in double strands [56]), but the perpendicular distance between the base planes generally shows little variation for two bases in the electronic ground state and is similar to the distance of closest approach between two aromatic molecules (3.4 Å in double-stranded B-DNA). It is also necessary to specify the torsion angle between a vector lying in the plane of one base, and a second vector in the plane of the second base. This torsion angle specifies the rotational setting or 'twist' between the stacked bases.

Each nucleobase also has distinguishable faces resembling the two sides of a coin [57], and it is necessary to specify which of the two distinguishable faces of each nucleobase is oriented toward the other base. This latter information is generally overlooked because stacking in regular double-stranded DNA is face-to-back, but face-to-face and back-to-back stacking motifs are possible in aggregates and in model single strands with flexible, modified linkers [58]. Unfortunately,

the nomenclature used in the literature is frequently ambiguous or contradictory and careful inspection is needed to determine the actual structure. For example, references to face-to-face motifs in [59] are more properly described as face-to-back stacks with a fully eclipsed geometry (twist angle of 0°).

Calculations of intrinsic (gas-phase) stacking energies have considered mostly face-to-back stacks (the stacking motif found in duplex DNA) and investigators have often ignored the possibility of face-to-face stacks [60]. For example, Florián et al. in their study of nucleobase dimers only performed calculations for face-to-back dimers, and assumed that face-to-face dimers are less stable [61]. This may be incorrect for systems with modified linkers or no linkers (aggregates). In fact, a face-to-face dimer is predicted to be the global minimum energy structure for a uracil–uracil stack [60]. It is important to search for both face-to-back and face-to-face stacks and careful selection of the base stacking coordinate may help achieve this goal [62].

Base stacks in B-DNA have a right-handed twist angle (Fig. 2), but this is by no means the only possible conformation. In the gas phase, an antiparallel alignment of the permanent dipole moments of each base minimizes dipole–dipole repulsion, but in solution a parallel alignment is preferred in order to maximize the solvation energy, which varies as the square of the total dipole moment in the Onsager model [60, 61]. Overall, the electrostatic energy of two stacked bases in the gas phase is acutely sensitive to the twist angle, but solvent screening greatly reduces this sensitivity [61, 63, 64]. Calculations indicate that the interaction energy of two stacked bases in aqueous solution depends only very weakly on the twist angle between the bases as long as there is at least some overlap between their π faces [61].

Differences in stacking free energies between the gas phase and aqueous solution are a reminder that water is critically important for stabilizing base stacks. At the low concentrations (several mM) used in most ultrafast laser experiments, nucleobase monomers will aggregate or self-associate in stacks of two or more bases instead of forming hydrogen bonds with each other [65, 66]. Self-association by hydrogen bonding does occur for the guanosine mononucleotide, but only becomes important at high concentrations above 100 mM [67]. In solvent-free (gas-phase) conditions, or in low polarity solvents [68–71], bases preferentially form base pairs. In the gas phase, two adenine molecules form a hydrogen-bonded base pair [16, 72], but blocking hydrogen-bonding sites by methylation leads to base stacks [72, 73]. Interestingly, clustering with only a few water molecules is sufficient to transform the A–A base pair into a stack [16]. Hydrogen bonding between ribose groups of nucleosides in the gas phase may also favor stacking [73].

In the end, base stacking in solution results from a delicate balance of forces between the intrinsic or *in vacuo* stacking energy and hydrophobic interactions [61, 64, 74]. The interaction is enthalpy driven, yet hydrophobic [75]. Stacking is exothermic ($\Delta H < 0$) but entropically disfavored ($\Delta S < 0$) such that stacked structures are preferred at low temperature, but bases unstack as the temperature is raised. Traditionally, NMR, CD, and UV hypochromism have been used to quantify the fraction of stacked bases in dinucleotides by fitting temperature-dependent

measurements to a two-state model in which the two bases are either stacked or unstacked [76–78].

These experiments reveal that base-stacked structures of dinucleotides are only weakly stabilized near room temperature. For example, stacks formed by two adenines, the canonical base with the greatest propensity for stacking [79], are stabilized by a ΔG of only about -0.9 kcal mol^{-1}. For dApdA, the fraction of stacked dinucleotides at 25°C is approximately 80% (reviewed in [58]). The weakness of this interaction means that a distribution of stacked conformers exists in aqueous solution. Although the backbone probably influences the kinds of stacked geometries that are preferred, it does not appear to influence significantly the stability of DNA base stacks.

3.2 Base Pairing

Base pairing is the association of two nucleobases by hydrogen bonding. The familiar Watson–Crick (WC) base pairs found in double-stranded DNA are sized such that the distance between the C1′ atoms of sugars on opposite strands is the same for A·T and G·C base pairs [80]. This enables any sequence of base pairs to fit into the double helix structure without distortion. Non-WC base pairing motifs are also important, particularly in RNA. Two non-WC motifs, important in model systems which have been the subject of photophysical investigations [81–86], are shown in Fig. 3.

Although it is straightforward to study single-stranded model compounds containing only stacked bases, no model system has been found which allows single base pairs to form in water, although they can be investigated in non-aqueous solvents (see Sect. 5.1). Instead, base stacking appears to be the inevitable companion of base pairing in aqueous solution. As discussed in Sect. 5, the simultaneous presence of base stacking and base pairing interactions in aqueous solution has made it difficult to isolate effects on photophysics from interbase hydrogen bonds. One effect which has come into focus recently is VC following ultrafast IC. In a base pair, hydrogen bonds to one or more solvent molecules are replaced by hydrogen bonds which join functional groups on the two bases. Base pairing thus reduces the number of hydrogen bonds that can be formed with water molecules. As discussed in Sect. 5.2.1, this can retard the rate of VC by slowing intermolecular vibrational energy transfer from the UV-excited chromophore to the surrounding water molecules.

3.3 Structural Complexity and Disorder

Complexity and disorder are two other traits of nucleic acids in room-temperature aqueous solution. A given base in a natural DNA or RNA strand is generally flanked

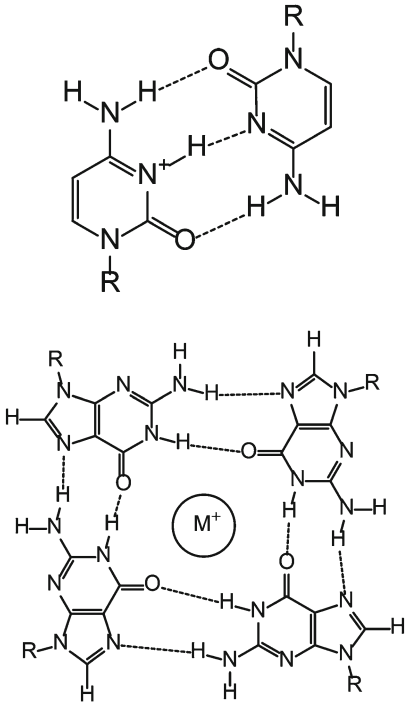

Fig. 3 Example non-WC base paired motifs found in DNA model systems that have been studied by ultrafast laser spectroscopy [81–86]. *Top*: Hemi-protonated CC base pair in which two cytosines share a single proton. *Bottom*: The G-quadruplex motif in which four guanines self-assemble around a central metal ion. *Dashed lines* indicate hydrogen bonds

by any one of four bases. The presence of minor bases such as 5-methylcytosine and 5-hydroxycytosine in DNA or any of the RNA minor bases further increases the number of possible nearest-neighbor bases. The consequences of this complexity for excited-state dynamics [87] can be explored, at least in principle, by performing (a possibly large number of) experiments on DNA oligonucleotides of appropriate sequence. More insidious is the conformational complexity which results in large numbers of structures of comparable free energy in solution – structures which may be poorly understood.

Conformational heterogeneity is manifest in different ways. In dinucleotides, stacked and unstacked bases can co-exist in equilibrium, but the stacked structures may be characterized by broad distributions of structures in which the twist angle and the stacking motif (face-to-face, face-to-back, etc.) are variables. In single strands, a wide variety of experimental techniques provide clear evidence that bases in single-stranded DNA and RNA sequences can stack with nearest neighbors [51, 88–90]. The question arises whether stacking by two bases affects the probability that a third base will stack on either end. Experimental consensus is that base stacking is mostly non-cooperative in single strands [91]. The lack of cooperativity is responsible for the broad UV melting curves observed for DNA single strands. An important consequence of non-cooperative base stacking is that the average length of stacked domains in a single-stranded oligonucleotide such as $(dA)_n$ can be quite short, even though the majority of bases are stacked with neighbors

[9, 91]. Consequently, the room-temperature structure of an oligonucleotide such as $(dA)_n$ in aqueous solution is thought to be similar to that of a rod–coil multiblock copolymer made of many short helical domains [51, 91, 92]. In Sect. 4.2.2 we argue that this stacking disorder, and not exciton delocalization, is responsible for the systematic variation in the amplitudes of fs-TA signals.

Base pairing can introduce further structural disorder. For example, base pairs near the terminus of a DNA strand open more readily than interior base pairs, an effect known as end fraying (see structure **1** in Fig. 12). Based on the rate of exchange of imino protons measured in NMR experiments, Guéron and coworkers concluded that the dissociation constant describing base pair opening of the terminal AT base pair in a self-complementary DNA octamer is 0.6 at 0°C [93]. This is higher by a factor of 40 than for a terminal GC base pair, which has three hydrogen bonds vs the two found in the AT base pair. A second kind of disorder concerns the ensemble of double-stranded structures which may be present in aqueous solution. The repetitive base sequences found in the AT-rich systems such as $(dA)_{18} \cdot (dT)_{18}$ and the alternating duplex $(dAdT)_9 \cdot (dAdT)_9$ which have been favorite systems for ultrafast laser investigations have relatively low melting temperatures and can undergo strand slippage (structure **2** in Fig. 12).

Complexity is also present in the form of structures that may not be anticipated from the secondary-structure elements found in regular B-DNA. For example, G- and C-rich sequences can spontaneously fold into G-quadruplex [94] and i-motif [95, 96] structures, respectively. The non-canonical base pairs that occur in these structures are shown in Fig. 3. Excited-state dynamics in novel DNA structures such as these will not be discussed here, but can be read about elsewhere [81–86]. Knowledge of the many ways that DNA can self-assemble into higher-order structures is clearly needed to interpret spectroscopic experiments correctly, which putatively investigate ‘standard’ single and double strands. For example, $(dG)_n$ sequences cannot be used to study G-on-G stacking in single strands because they will form G quadruplex structures in room-temperature aqueous solution [97].

3.4 Electronic Structure

Having introduced some basic structural characteristics of nucleic acids, we end this section with an overview of the types of excited electronic states found in DNA. In a multichromophoric molecule such as DNA, the singlet $\pi\pi^*$ and $n\pi^*$ states of single bases can interact to form new, delocalized excitations that span two or more bases. The electronic coupling which gives rise to these new states is sensitive to interbase separation and orientation. For this reason, spatial structure profoundly influences electronic structure in DNA.

Delocalized excitations can be approximately categorized as Frenkel excitons or charge transfer (CT) states, but mixing between these limiting cases is also possible [98, 99]. The former are neutral excited states which result from excitation resonance between degenerate or nearly degenerate transitions located on two or more

bases. When the coupled chromophores are separated by more than about 6 Å, relatively long-range electrostatic coupling between transition dipole moments of energetically similar transitions gives rise to Frenkel excitons [100–102]. At shorter intermolecular distances, there are major contributions to the electronic coupling from orbital-orbital overlap, and excimer (exciplex) states can be formed [103].

Although exciton is a general term frequently used to denote *any* excited state in a multichromophoric system, we will use exciton hereafter as a synonym for 'Frenkel exciton,' following common usage in the field. It should be kept in mind that 'excimer' (=excited dimer) and 'exciplex' (=excited complex) are similarly generic terms which in principal apply to any excited state of two chromophores with significant orbital-orbital overlap. Such states exist on a continuum running from contact ion pairs generated by the transfer of a full electron between molecules to states with strong mixing from locally excited or excitonic states [104]. Strong and short-range interactions can also lead to covalent bond formation in the excited state in both excimers and exciplexes [59, 105–108]. Clearly, anyone hoping for a completely unambiguous specification of the character of an excited state involving two chromophores will be disappointed by these terms. We will use excimer and exciplex hereafter, as they are used widely in the literature, but we shall also supplement them with terms such as 'ion pair state,' 'CT state,' and 'bonded excimer,' as appropriate, to provide additional description about an excimer state when this information is available either from experiment or calculations.

A full understanding of excited-state dynamics in DNA requires knowledge of the nature, spatial extent, lifetimes, and yields of excited states created by UV radiation. Of interest are the states reached in absorption and excited states not populated initially, but which are decay intermediates. Sections 4 and 5 explore these 'intermediate' excited states in detail. Here, we summarize briefly what is known about the excited states populated by UV absorption. Theory indicates that excitons in assemblies of bases can be delocalized over as many as two to three bases [40, 109]. They constitute a dense band of states which are affected by conformational disorder and homogeneous broadening, and which can vary widely in oscillator strength [110, 111] The strong absorption by DNA strands at UVB and especially UVC wavelengths arises overwhelmingly from bright excitonic states with little contribution from CT states on account of the low oscillator strength of the latter states [112]. Markovitsi and coworkers have argued that the very weak tail absorption by DNA oligonucleotides in the UVA spectral region is caused by direct excitation of weak CT states [17, 113]. At wavelengths longer than 320 nm, the molar absorption coefficient per base is typically not much greater than 10 M^{-1} cm^{-1}. Even though the CT states lie above the lowest energy excitons at the ground state geometry (see Sect. 4.1.5), greater inhomogeneous broadening is proposed to make them the only absorbers above 320 nm. Motivated by interest in UVA photochemistry by DNA, a few studies have appeared on the UVA spectroscopy of DNA [17, 113], but our focus in the remaining sections will be on experiments performed with UVB/UVC excitation. For such studies, the initial excited states are excitons.

4 Excited-State Dynamics in Single Strands

In this section, we consider excited states in single strands of DNA in which the nucleobases stack with one another, but lack interbase hydrogen bonds. Strikingly, a substantial fraction of excited states formed in single strands relax orders of magnitude more slowly than those of single bases (Fig. 4). These states, which appear in model compounds with two or more π-stacked bases, are referred to as long-lived excited states [1, 4, 13, 22, 23, 27, 87, 114–123] to contrast them with the subpicosecond excited states of the nucleobase monomers. Prominent long-lived signal components, with lifetimes of between a few and several hundred picoseconds, are seen in GSA and ESA signals recorded in fs-TA experiments, as discussed below. Even longer-lived states have been observed, especially using the sensitive TCSPC technique, although the quantum efficiency for reaching these states appears to be very low at UVB and UVC wavelengths. Confusingly, "long-lived" tends to mean "10–200 ps" in the literature describing fs-TA experiments (e.g., in [9]), while it generally means ">1 ns" in papers discussing fluorescence decay curves measured with the TCSPC technique (e.g., in [124]). The difference arises from the longest time scales that can be readily probed by the respective techniques. Consequently, comparisons should be made cautiously.

Long-lived excited states were first seen in fs-TA measurements on the single-stranded homopolymers poly(A) and poly(dA) [27]. This study showed that raising the temperature reduces the magnitude of the long-lived signal component (τ ~154 ps). The attenuation of the long-lived signal at high temperature was interpreted to mean that these states are formed in base stacks because base stacking is progressively disrupted at elevated temperature [125, 126].

Later experiments showed that essentially identical long-time signals are observed in the dinucleotide ApA and in the much longer homopolymer poly (A) [6], suggesting that the long-lived excited states have a spatial extent of no more than two bases. Dinucleotides (i.e., dinucleoside monophosphate compounds in which just two bases are joined by a phosphodiester linkage; see structure of dApdA in Fig. 4) are minimal-length single strands, which have taken on great importance in studies of DNA excited states. For this reason, we begin by discussing the excited-state dynamics of dinucleotides in detail, along with pertinent electronic structure calculations, before discussing excitations in single strands with more than two bases.

4.1 Dinucleotides

4.1.1 Long-Lived Excited States Form Only in Base Stacks

Compelling evidence that long-lived excited states are only formed when two bases are in van der Waals contact comes from experiments showing that these states

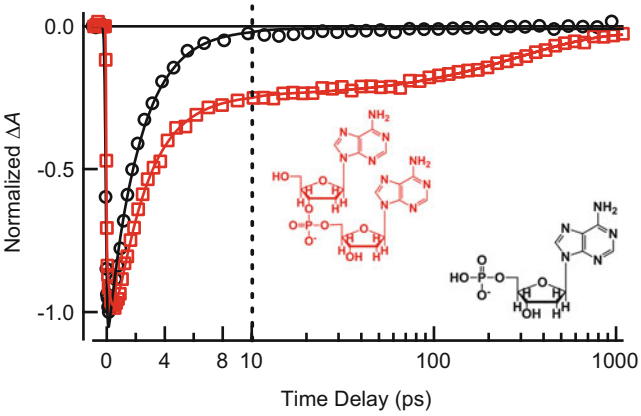

Fig. 4 fs-TA signals (266 nm pump/250 nm probe) in aqueous buffer solution: dAMP in *black* and dApdA in *red*

disappear when base stacking is eliminated. At low pH, each residue in dApdA is protonated and Coulombic repulsion completely disrupts stacking [127–129]. GSB recovery signals (pump 265 nm/probe 250 nm) show no long-lived signal for this fully unstacked structure, whereas a long-lived component with a decay time constant of ~200 ps is seen at neutral pH (Fig. 5) [9]. Protonation does not inhibit ultrafast IC, as evidenced by the identical GSB signals at pH 2 and pH 7 for dAMP [9].

Notably, long-lived excited states are still observed at low pH in poly(A) [27] and poly(dC) [81], conditions under which the polymers adopt higher-order structures which retain base stacking. This suggests that it is not protonation of the nucleobases per se that quenches long-lived excited states, but rather the loss of base stacking. This conclusion is underscored by the observation that high concentrations of methanol, a known denaturant, also causes unstacking and eliminates the long-lived excited states seen in fs-TA experiments on AA nucleobase dimers (see Sect. 4.1.6) [58].

4.1.2 Long-Lived Excited States Are Assigned to Excimers

The prominent decay components seen in fs-TA signals of $(dA)_{18}$ in aqueous solution were assigned by Crespo-Hernández et al. [13] to intrastrand excimers. Later experiments [6, 9] detected identical signals from dinucleotides and longer oligomers made of adenine (see Sect. 4.2.1), providing strong evidence that the long-lived excited states are indeed localized on just two nucleobases, as required for an excimer (=excited dimer). Time-resolved fluorescence experiments detected similar decay components in emission, both in dinucleotides [122, 130] and in longer single strands [23]. This emission is significantly red-shifted compared to that from the constituent monomers, and this observation is again consistent with

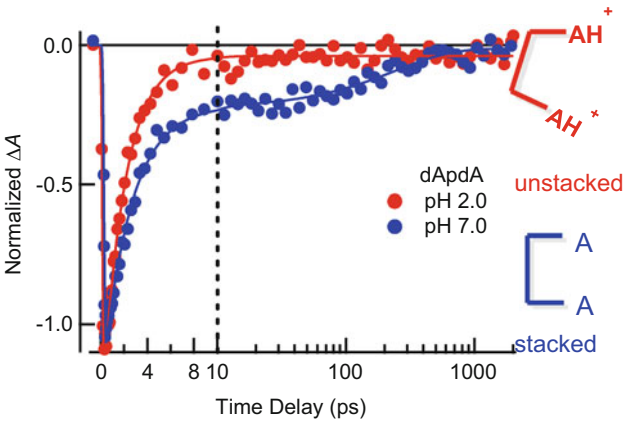

Fig. 5 fs-TA signals (266 nm pump/250 nm probe) of dApdA at pH 2 (*red*) and pH 7 (*blue*). Figure adapted from [9]

excimer formation. The finding from ultrafast laser experiments that excimers are important excited states in DNA model compounds at room temperature supports the assignment made in the 1960s of red-shifted emission seen from dinucleotides and longer DNA strands in rigid glasses at cryogenic temperatures to excimer states [131].

Alternative assignments for the long-lived excited states have been discussed [116, 132–134]. Several workers proposed that the ultrafast IC observed in the nucleobase monomers could be impeded in π-stacked systems because of steric hindrance of the out-of-plane vibrational modes that facilitate IC [116, 133–135]. However, the steric explanation is hard to reconcile with the sequence-dependent lifetimes observed in dinucleotides [6]. Presently, there is growing experimental and theoretical consensus that excited states seen in single DNA strands which decay with time constants of tens to hundreds of picoseconds are excimers [13, 23, 59, 108, 121, 122]. Evidence that these excimers have a high degree of CT character is discussed next.

4.1.3 DNA Excimers and Interbase Charge Transfer

Takaya et al. [6] reported that excimer decay rates measured by fs-TA spectroscopy in a series of RNA dinucleotides increase as the estimated energy of the radical ion pair generated by interbase electron transfer decreases. This correlation suggested that UV excitation of a stack of neutral bases produces CT states which decay by charge recombination at rates that decrease with increasing thermodynamic driving force (Marcus-inverted behavior) [6].

Very recently, direct evidence has been obtained by fs-TRIR spectroscopy that some DNA excimers exhibit the vibrational spectral features expected of radical ion pairs generated by interbase electron transfer [123, 136, 137]. By probing the

double-bond stretching region after photoexcitation of the dinucleotide dApdT, Doorley et al. [123] observed a 75-ps component with excited-state absorption features between 1,500 and 1,600 cm^{-1}. By comparing the calculated shift of the C=O stretching modes of the neutral thymine molecule and the thymine radical anion, the authors argued that this relatively broad feature can be assigned to the thymine radical anion formed by electron transfer from A to T.

Bucher et al. [136] observed slow decay components in fs-TRIR signals from di- and oligonucleotides containing 5-methylcytosine. The long-lived excited states have lifetimes of 20–300 ps and are formed in 20–40% yield. These components are furthermore absent in equimolar mixtures of the corresponding monomers. The authors assigned their mid-IR ESA bands to radical cations and anions generated by photoinduced charge separation. These assignments were supported by transient IR difference spectra of authentic radical cations of guanine and 5-methylcytosine generated by two-photon ionization. Additionally, ab initio calculations identified vibrational marker bands of the radical anions. Bucher et al. concluded that CT states formed in single strands containing more than two bases can delocalize across multiple stacked bases. This fascinating proposal will be discussed further in Sect. 4.2.2.

Finally, Zhang et al. [137] used fs-TRIR spectroscopy to study the dinucleotide d(OA) (structure shown in Fig. 6), where O stands for the modified nucleobase, 8-oxo-7,8-dihydro-2′-deoxyguanosine (8-oxo-dGuo, or O in sequences). The TRIR spectra of d(OA) at various delay times are shown in Fig. 6a. The difference spectra recorded between $30 \leq t \leq 300$ ps match the theoretical difference spectrum calculated for an ion pair consisting of an 8-oxo-dGuo radical cation and an adenine radical anion (Fig. 6b). This is a clear demonstration that an electron is transferred from the 8-oxo-dGuo residue to A, producing an exciplex best described as a strong CT state or even a contact radical ion pair. The quantum yield of forming the CT state is high and equal to 40% at 265 nm, but decreases to 10% at 295 nm, a wavelength which selectively excites 8-oxo-dGuo [137].

The potentially reactive radical ions formed in d(OA) decay to the ground state of the dinucleotide by charge recombination with a time constant of 60 ps. Ultrafast ET between π-stacked bases possibly explains how 8-oxo-dGuo can contribute to the reductive repair of thymine dimers in DNA [138] despite its ultrashort monomer lifetime [139]. The requirement that the bases must be stacked at the instant of photon absorption in order to form a radical ion pair also explains why a photoexcited purine base (A or G) cannot repair a flanking CPD when the bases are unstacked [140].

In summary, transient IR difference spectra providing direct evidence of interbase electron transfer have been measured recently in three laboratories for dinucleotides [123, 136, 137] and longer single strands [136]. It was assumed in each study that a full electron is transferred between π-stacked bases, but the question of whether an excimer with a reduced degree of CT character would have similar vibrational frequencies as a contact radical ion pair has not been explored. Also, although a crude estimate using aqueous reduction potentials suggests that ion pairs can be formed for any dimer made of the canonical

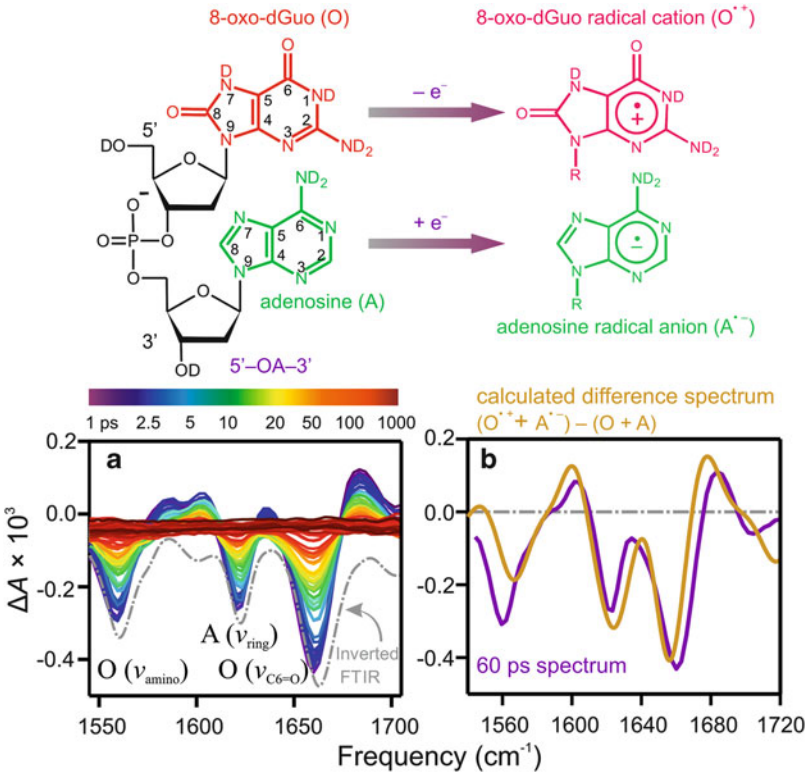

Fig. 6 (**a**) fs-TRIR spectra of d(OA) at selected pump-probe delay times (1 ps–1 ns) following 265 nm excitation. The Inverted FTIR spectrum and mode assignments are included for convenience. (**b**) The experimental difference spectrum at 60 ps (*purple line*), compared with the difference spectrum calculated as $(O^{\bullet+} + A^{\bullet-}) - (O + A)$ (*gold line*). The DFT calculations were performed at the PCM/PBE0/6-31 + G(d,p) level of theory and using the harmonic approximation for the monomeric species with 2′-deoxyribose and five explicit D_2O molecules included. The structures of d(OA), $O^{\bullet+}$ and $A^{\bullet-}$ are also shown. Figure adapted from [137]

nucleobases [137], it is unknown whether full electron transfer occurs in homodimers such as $(dA)_2$, or whether these form excimers with a reduced degree of CT character. Calculations discussed in Sect. 4.1.5 have predicted the existence of both types of excimers in AA stacks.

4.1.4 Initial Excitons Decay to Excimers

An important observation from fs-TA and TRIR experiments is that a large fraction of all initial excited states decay to excimers [9, 13, 136, 137]. An analysis of GSB signals recorded with 266-nm pump pulses found that ~30% of all excited states in $(dA)_2$ in room-temperature aqueous solution decay to excimers [9]. Bucher et al. [136] concluded that 25% of excited states in the dinucleotide d(^{5m}CA),

where ^{5m}C is 5-methylcytosine, decay to excimers. Considering that unstacked conformations cannot form excimers (Sect. 4.1.1), the probability of excimer/exciplex formation is even higher for excitations in base stacks.

The observation of high excimer yields has important implications regarding their nature. If the excimers were as bright in emission as the $^1\pi\pi^*$ states of the mononucleotides, then the high yields and long lifetimes of the excimers would cause the fluorescence quantum yields of the dinucleotides to increase by orders of magnitude, but this is not observed. For example, the AA excimer, which may be one of the brightest of DNA excimers, causes the fluorescence quantum yield of $(dA)_{20}$ ($\phi_f = 6 \times 10^{-4}$ [17]) to increase by just an order of magnitude compared to dAMP ($\phi_f = 6.8 \times 10^{-5}$ [141]), even though the oligomer lifetime is ~1,000 times longer. This comparison and the very weak nature of the long-time emission [23, 122, 130] – a circumstance that made it difficult to even detect long-lived excited states by the fs-FU technique at first (see discussion in [4]) – indicates that the long-lived excited states are comparatively dark, and have lower radiative transition rates than the bright $\pi\pi^*$ states of the monomers. This is fully consistent with the strong CT character described in the previous section. It is important to note that the excimer states are not completely dark, as decay components are observed in time-resolved fluorescence experiments closely matching those found in fs-TA experiments in dinucleotides [122, 130] and longer single strands [23].

A variety of experiments suggest that excimers or CT states are populated in less than 1 ps from the initial excitons [6, 13]. For example, Zhang et al. [137] observed that the CT state yield in d(OA) is four times higher at 265 nm than at 295 nm. This suggests that there is greater coupling between the initial excitonic state and the CT state at 265 nm and ultrafast transfer from the former to the latter. In addition, the excimers emit at wavelengths to the red of the base monomers, but rising emission signals have not been observed at these longer wavelengths (or at any emission wavelength) in fs-FU experiments [122, 130]. The paradigm in which excitons decay on an ultrafast time scale to excimer or CT states is also supported by computational studies [108, 142]. For example, quantum dynamical calculations predict that IC from excitonic to CT states can occur in less than 100 fs in adenine single strands containing between two and ten bases [143].

4.1.5 Computational Predictions and Multiple Excimers

The principal findings from calculations of excited states of π-stacked nucleobase dimers are briefly reviewed in this section, focusing on the A–A dimer, the most studied system and one of special relevance to fs-TA experiments on single strands. These calculations provide insight into the exciton-to-excimer decay mechanism introduced above. Considerable computational effort has been devoted to locating the vertical energies of CT states within the manifold of excited states, and here we present a small number of conclusions from only a few representative studies. Accurate ab initio prediction of excited state energies is enormously challenging because of the large number of atoms and the desire to include realistic solvation

models. System size frequently makes it prohibitively expensive to use higher levels of theory. Because of their efficiency, DFT calculations are popular, but this method can predict spuriously low energies for CT states [144] unless suitable long-range corrected functionals are used [145, 146].

TD-DFT studies of the π-stacked adenine dimer by Lange and Herbert using long-range corrected functionals [147], of stacked adenine–guanine systems by Santoro et al. [117], and a study of adenine multimers with the ribose-phosphate backbone included by Improta and Barone [108] predict that the CT states lie within about 0.3 eV of the bright excitonic states at the geometry of the electronic ground state. These TD-DFT results are roughly in line with ab initio CASPT2 calculations performed on the π-stacked adenine dimer, which predict that the CT states are 0.1–0.3 eV above the lowest lying excitonic state [59]. Plasser and Lischka computed the excited-state properties of a stacked adenine dimer using the RI-ADC(2) method [120]. These supermolecule ab initio calculations, which treat CT and excitonic states on an equal footing, revealed that CT states lie 0.6–0.8 eV above the bright excitonic states. Accurate equation of motion coupled-cluster calculations have since narrowed the gap somewhat between the bright ππ* states and the lowest CT state [148].

Although the CT excited state for AA lies vertically above the lowest energy excitons, what counts is whether there is an accessible pathway leading from the Franck–Condon region to the CT state. Computational studies which performed excited-state geometry optimization confirm that such paths exist [107, 108]. A recent quantum dynamical investigation furthermore suggests that this interconversion can occur on an ultrafast time scale [143]. In summary, a growing number of computational studies support the concept that decay of single strand excitons to excimers is energetically feasible and occurs on an ultrafast time scale.

An important contribution from theory is the location of more than one type of excimer minimum on the potential energy hypersurface of AA stacks [59, 108, 121]. The suggestion that two excimers are formed in UV-excited $(dA)_{20}$ was originally made by Kwok et al. [23]. Ab initio calculations of excited states of stacked adenine dimers identified a neutral excimer with an eclipsed geometry (twist angle of 0°), which is characterized by short C4–C4′ and C5–C5′ distances [59, 108]. Plasser and Lischka [120] also describe a geometry-optimized excimer state (termed an exciplex state in [120]) with a very short distance of 2.00 Å between the C6 atoms of each adenine. The resulting strong orbital interaction between the two adenines yields an excited state very different compared to the Franck–Condon state and it has character intermediate between a Frenkel exciton and a charge resonance state [120]. It will be important to see whether these predictions for adenine dimers extend to dinucleotides containing two different bases.

Large-scale backbone motions are required to bring two bases in B-form DNA into an eclipsed conformation. For this reason, it may be impossible to reach a fully eclipsed conformation in actual di- and oligonucleotides because of backbone constraints, and excimers having larger twist angles have been predicted

[108, 121]. Banyasz et al. [121] suggested that two different excimers can explain the trends in steady-state and time-resolved fluorescence spectra from adenine homo-oligonucleotides. In particular, they argued from their TCSPC experiments on $(dA)_{20}$ that the subnanosecond emission (λ_{em} ~360 nm) should be assigned to the "neutral excimer" (a bonded excimer), while nanosecond time scale and longer wavelength emission arises from an AA CT state which, in its energy-minimized geometry, has a stacking distance similar to that in the electronic ground state of the oligomer [121].

To support their assignment, Banyasz et al. [121] pointed out that the emission band at 360 nm seen for $(dA)_{20}$ is missing in the fluorescence spectrum of the $(dA)_{20}{\cdot}(dT)_{20}$ duplex. They proposed that the neutral excimer responsible for the subnanosecond emission decay in $(dA)_{20}$ is unable to form in duplex $(dA)_{20}{\cdot}(dT)_{20}$ because base pairing prevents the required torsional motions [121]. This explains the absence of any significant picosecond time scale emission from AT homoduplexes as reported in [40, 149], but this model leaves unresolved the nature of the excited states seen in fs-TA experiments for $(dA)_{18}{\cdot}(dT)_{18}$ and related homoduplexes that decay with a lifetime of ~70 ps (see Sect. 5.2.1).

Temps and coworkers [130] invoked the fully eclipsed excimer geometry calculated by Olaso-González et al. [59] to interpret the ~5 and ~280 ps decay components observed in their fs-FU experiments on the dinucleotide d(pApA). They proposed that an initial excimer is formed with a twist angle of ~36° between the bases (corresponding to the initial geometry in the B-DNA helix), which decays in 5 ps to a more stable, eclipsed (twist = 0°) excimer. They assigned the 280-ps lifetime to the latter species. A similar model was discussed in a later study of d(ApG) [122]. In that study, a ~6-ps component was again observed at red-shifted wavelengths in the fluorescence signal. Its absence in a GSB recovery measurement is consistent with a model in which less stable excimers decay to more stable ones as bases undergo large amplitude motions.

However, proof is lacking that the minimum energy excimer or exciplex actually corresponds to a structure with zero twist. In addition, it has not been demonstrated that the requisite large-amplitude twisting motions can actually be completed on a 5–6 ps time scale. After all, reorientational diffusion of a single adenosine molecule occurs more slowly. An alternative explanation is that the energy of the emitting excimer state is progressively lowered by changes in the environment. This possibility is suggested by spectral changes seen in the emission spectrum of $(dA)_{20}$ [130] which could be described as a continuous red shifting on the few picosecond time scale. Although solvation dynamics in neat water are largely complete in less than 1 ps [150], significantly slower solvation times have been reported for chromophores embedded in DNA [151, 152].

4.1.6 Excimer Lifetimes and Stacking Geometry

Several diadenosine compounds (Fig. 7) were studied by fs-TA and steady-state (UV/vis, CD) spectroscopy in order to explore the effects of (1) temperature,

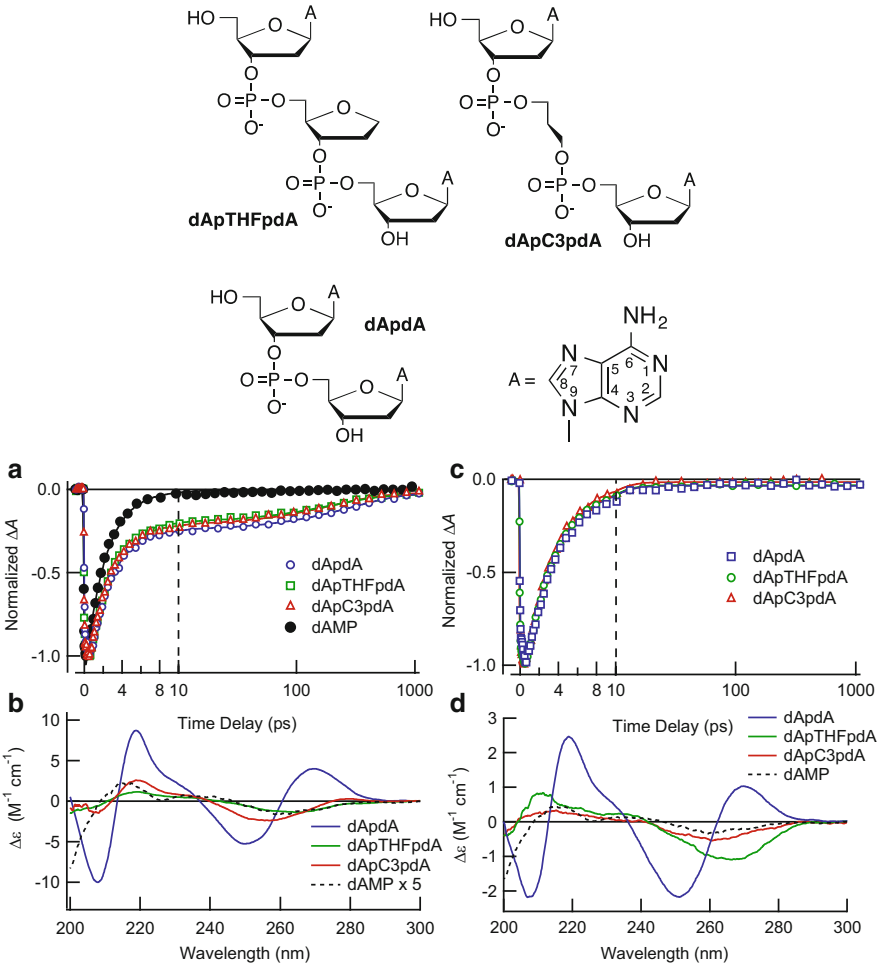

Fig. 7 *Top*: Structures of the 2′-deoxyadenosine dimers studied. *Bottom*: fs-TA signals (266 nm pump/250 nm probe) and CD spectra in buffered aqueous solution (**a**, **b**) and in 80 vol% methanol:20 vol% buffer (**c**, **d**)

(2) solvent composition, and (3) the nature of the covalent linker joining the nucleobases on excited-state dynamics [58]. Dimers of (2′-deoxy)adenosine were chosen because of adenine's high stacking propensity in aqueous solution [43, 153, 154]. A pronounced long-lived component is observed in all three 2′-deoxyadenosine dimers which is not seen in the pump-probe signal of the monomer dAMP (Fig. 7a). This signal component vanishes completely in 80 vol% methanol/20 vol% water (Fig. 7c). Methanol was used in this study as a denaturing co-solvent to disrupt π–π stacking of the adenine moieties. The exciton-coupled circular dichroism (ECCD) spectra indicate that the 2′-deoxyadenosine

units remain stacked most of the time in aqueous solution (Fig. 7b), while few, if any, stacked structures are present in aqueous methanol (Fig. 7d).

When two 2′-deoxyadenosines are separated by an abasic site (dApTHFpdA and dApC3pdA in Fig. 7), the bases stack just as readily as when they are nearest neighbors, yet these compounds show no ECCD signals (Fig. 7b). Low barriers to helix inversion for diadenosines joined by longer linkers may produce a racemic ensemble in which left- and right-handed helical conformations are in dynamic equilibrium [58]. These results caution that a CD spectrum resembling that of a monomer (i.e., one that lacks excitonic interactions) is not a foolproof indicator of unstacked conformations [58].

Even though the bases in dApdA adopt an extended conformation in 80% methanol, as indicated by the lack of a long-lived component in the fs-TA signal (Fig. 7c), the ECCD signal is not fully eliminated (Fig. 7d). This indicates that an ECCD signal does not always imply base stacking. In their computational study of ECCD by the RNA dinucleotide ApA, Johnson et al. [155] identified a conformation with perpendicularly oriented base planes for which the calculated CD signal was only 20% as intense, but otherwise had the same spectral shape as the calculated CD spectrum of a co-facially stacked conformer with B-DNA geometry. An open conformation with intervening solvent molecules can thus lack the orbital-orbital overlap necessary for excimer formation, but still yield an ECCD spectrum, perhaps because the short phosphodiester linker constrains the two bases in dApdA to adopt unstacked conformations that are predominantly chiral.

The absence of base stacking in aqueous methanol is a reminder that hydrophobic interactions are critically important for stabilizing base stacks [154, 156]. In most nonaqueous solvents, dinucleotides adopt unfolded conformations in which the bases have no overlap between their π orbitals and are separated by solvent molecules. Interestingly, extended, unstacked conformations were not observed in a molecular dynamics (MD) simulation of ApA in methanol [157]. This discrepancy with experiment adds to evidence that the empirical force fields used in MD simulations overstabilize base stacking in single-stranded systems [54, 55, 158].

High concentrations of methanol disrupt base stacking more effectively than high temperature conditions (Fig. 8). Increasing the percentage of methanol causes the signature of the excimer state in the fs-TA signals from dApdA to decrease in amplitude, and eventually disappear above 50% methanol concentration (Fig. 8b). Increasing temperature in aqueous solution also leads to attenuation of the slow decay component, but the fs-TA signal recorded at the highest temperature still exhibits a long-lived decay (Fig. 8a). The detection of excimers in dApdA at 75°C confirms that there is still substantial AA base stacking at high temperature. Earlier, Davis and Tinoco concluded from NMR measurements that the two bases in ApA remain close to each other with no solvent molecules in between most of the time, even at 90°C [159].

Two 5′,5′-linked diadenosine oligophosphates P^1,P^4-di(adenosine-5′) tetraphosphate (Ap_4A) and P^1,P^5-di(adenosine-5′)pentaphosphate (Ap_5A) were also studied by fs-TA and CD (Fig. 9). Previous studies suggested that these compounds adopt non-face-to-back stacking motifs [160, 161]. The long-

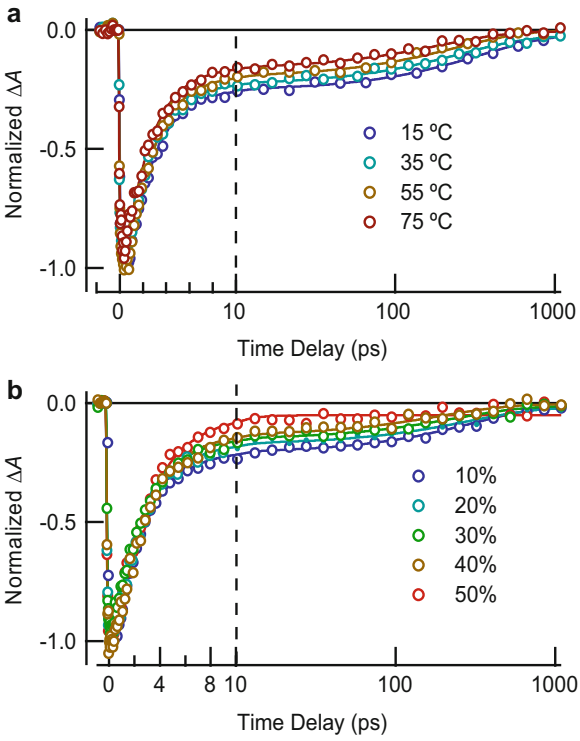

Fig. 8 fs-TA signals (266 nm/250 nm) from (**a**) dApdA at the indicated temperatures in aqueous buffer solution, and (**b**) in methanol–water solutions as a function of the percent methanol by volume

wavelength couplet seen in the ECCD spectra of Ap_4A and Ap_5A (Fig. 9b) is opposite in sign to the one seen in dApdA (Fig. 7b). This and other characteristics of the CD spectra are best explained by a face-to-face stacking motif. Interestingly, the fs-TA GSB signals (266 nm/250 nm) for these two dimers reveal that excimers are formed which have lifetimes similar to those seen in the 2′-deoxyadenosine dimers.

The main messages of the work described in [58] is that AA stacks form readily in substrates having very different backbones and excimers form in high yields in these stacks, despite the different distributions of ground-state conformations. The disappearance of long-lived fs-TA signals under conditions that still produce ECCD signals is evidence that the interactions between bases leading to excimer states are short-ranged [58]. The steep distance dependence that characterizes excimer formation is furthermore consistent with interbase electron transfer (see Sect. 4.1.3). It is well known that electron transfer rates decrease exponentially with donor–acceptor distance [162]. Excimer formation thus requires π−π stacking between nucleobases because this organization positions an electron donor and acceptor base close enough to make electron transfer competitive with the very high rate ($\sim 10^{13}$ s^{-1}) of IC observed in base monomers.

The very different ECCD spectra in Figs. 7 and 9 indicate that twist angles and stacking motifs (face-to-back, face-to-face, etc.) differ in these five adenine dimers with their different linkers. In spite of this variation, excimers are formed in all,

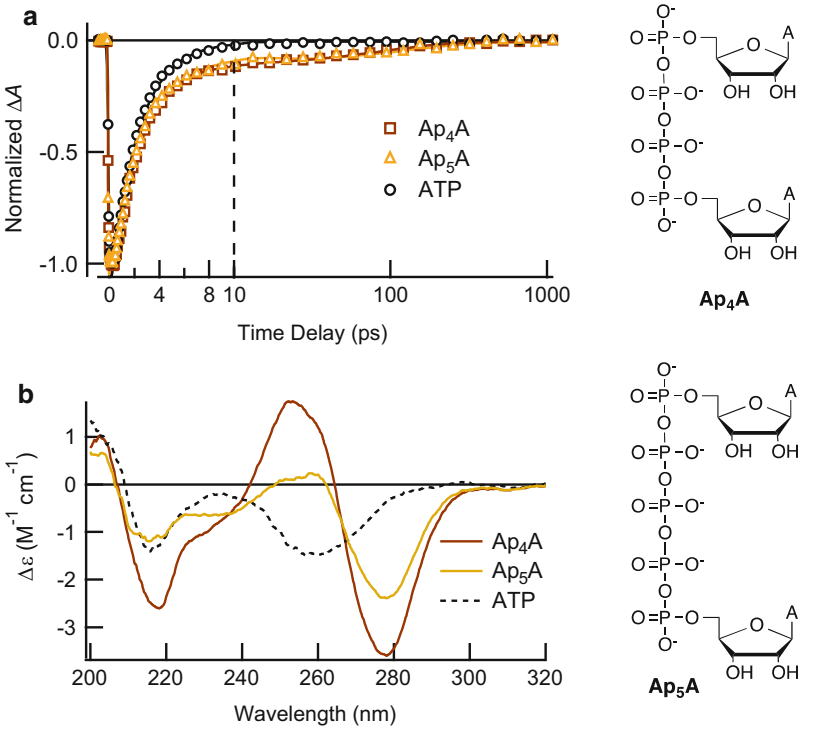

Fig. 9 (**a**) fs-TA signals (266 nm pump/250 nm probe) and (**b**) CD spectra in buffer solution of adenosine 5′-triphosphate (ATP), Ap_4A, and Ap_5A (structures shown at *right*)

which decay with remarkably similar, if not identical, lifetimes [58]. This could be because motions needed to reach a lowest energy excimer are largely complete in ~10 ps, the earliest time at which the AA excimer can be observed without interference from hot-ground state absorption following ultrafast IC by shorter-lived excited states [58].

It is, however, important to note that face-to-face (AA dimers in Fig. 9) and face-to-back stacks (AA dimers in Fig. 7) cannot achieve identical geometries without flipping over one of the bases, a motion thought to occur on subnanosecond time scales. This could indicate that the excimer state formed in high yield is not a neutral or bonded excimer [59, 107, 108, 163, 164], the energy and lifetime of which might be expected to depend sensitively on geometry. Instead, an excimer which is essentially a contact radical ion pair similar to those observed in d(OA) and other base heterodimers (Sect. 4.1.2) may be responsible. The energy of such an excimer could depend more weakly on twist angle and stacking motif.

4.2 Single-Stranded Oligonucleotides

An important observation from ultrafast laser experiments is that long-lived states are ubiquitous in DNA single strands, regardless of length. Comparison of dinucleotide signals with those from longer oligomers provides insight into the nature of the excited states and can be used to draw conclusions about excited-state localization.

4.2.1 Excimer Dynamics in Oligonucleotides

Experimental results from many laboratories have detected excimers in DNA oligonucleotides containing more than two bases. Experiments performed using the fs-TA technique on $(dA)_{18}$ [27], poly(A), and poly(dA) [13] all revealed a slow decay component of between 100 and 200 ps. Buchvarov et al. [132] observed long-lived excited states in a series of single-stranded homo-adenine oligomers in fs-TA experiments. Su et al. [9] also investigated variable-length dA homo-oligonucleotides using the UV pump/UV probe fs-TA technique. Their measured GSB signals (Fig. 10) show that long-lived excimers are formed in all oligonucleotides, regardless of length. Earlier, Takaya et al. [6] had observed that the RNA dinucleotide ApA and its corresponding homopolymer poly(A) have identical long-time signals in GSB experiments. The constancy of the long lifetime on going from $(dA)_2$ to $(dA)_{18}$ strongly suggests that the excitations probed in all strands are delocalized over no more than two π-stacked neighbors, consistent with excimer formation.

Time-resolved fluorescence experiments provide a slightly different perspective on the dynamics of the optically prepared exciton states. The emission anisotropy measured in fs-FU experiments decays on the femtosecond time scale for many single and double strands [124]. Markovitsi and coworkers assign this decay to IC ("energy transfer" or "intraband scattering") among excitonic states [124, 165]. However, the proposal from fs-TA experiments that excitons decay in $<$100 fs to excimer/exciplex states (Sect. 4.1.4) is a possible additional mechanism for the rapid anisotropy decay. The transition dipole moments of DNA excimers can be oriented out of the plane of the bases in contrast to the in-plane excitonic transition moments [120, 166]. Thus, femtosecond evolution from an exciton to an excimer state would lead to a rapid change in polarization anisotropy.

4.2.2 Exciton and Excimer Delocalization in Single-Stranded DNA

Using a novel approach, Buchvarov et al. [132] estimated the spatial extent of DNA excitons using fs-TA signal amplitudes recorded from variable-length adenine homo-oligonucleotides. By fitting the amplitudes as a function of the strand length, the authors estimated a "1/e delocalization length" of 3.3 ± 0.5 bases in $(dA)_n$

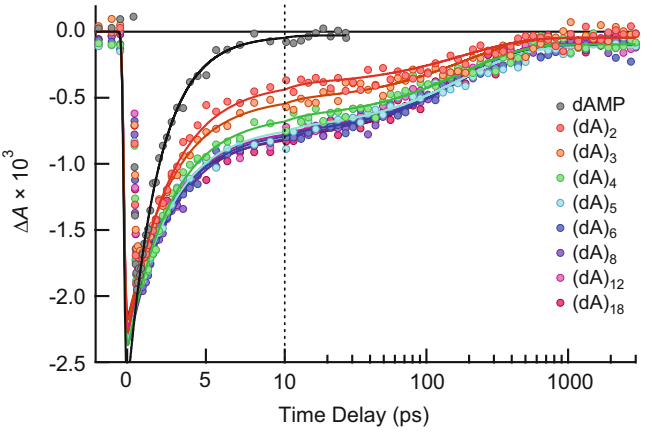

Fig. 10 fs-TA signals (266 nm pump/250 nm probe) of dAMP and adenine homo-oligonucleotides with 2 to 18 bases obtained with consecutive scans. Figure reused with permission from [9], copyright (2012) American Chemical Society

sequences, a result that implies greater exciton delocalization in the longer strands [132]. Interestingly, CD experiments also suggest that excitons can span more than two bases, but in a manner that depends on excitation wavelength. Nielsen and co-workers concluded that excitons prepared by photons with wavelengths above 220 nm extend over just two bases, while excitons prepared by VUV photons were suggested to spread over up to eight bases [167]. The compact, lower energy excitons are more relevant to the excitation conditions in the ultrafast laser experiments. In a computational study, Tonzani and Schatz [168] predicted a delocalization length of approximately three residues for single-stranded $(dA)_n$ oligomers containing between 7 and 11 bases.

Su et al. [9] reinvestigated $(dA)_n$ oligonucleotides by the fs-TA technique and showed that the GSB signals could be fitted to the same time constants regardless of length, and only the relative *amplitude* of the slow signal component increased with increasing strand length (Fig. 10) [9]. They argued that long-lived excitations in single strand adenine tracts are already fully localized excimers no later than 1 ps after excitation, and cast doubt on the possibility of using fs-TA signals recorded several picoseconds after excitation to reach conclusions about exciton delocalization, as was done in [132].

Su et al. [9] emphasized that structural disorder, specifically, the variation in the fraction of stacked bases with length, provides a better explanation of the amplitude variation seen in Fig. 10. They pointed out that the average length of stacked domains in ss DNAs is generally much less than the strand length [91]. In fact, these authors estimated that the average stacked domain in $(dA)_{18}$ is only 1.8 bases long, assuming that 69% of all bases in $(dA)_{18}$ are stacked near room temperature.

An interesting variation on the concept of delocalized excitons is the idea that CT (or excimer) states can delocalize across multiple stacked bases. Such states have been observed in calculations of double strands [147], and they are familiar

from work on DNA charge transport [169]. Bucher et al. [136] concluded from their fs-TRIR studies of DNA single strands that one or both of the radical ions produced by UV excitation can delocalize across multiple stacked bases. This conclusion is based on experiments in which 5-methylcytosine was selectively excited in a single strand that also contained an adenine positioned a variable distance away by intervening uracil bases. The observed bleaching of ground-state IR fundamentals of both the U and A bases led the authors to conclude that charge separation can extend over distances of 10 Å [136].

The identical GSB recovery dynamics observed by Su et al. [9] for $(dA)_2$ and $(dA)_{18}$ are difficult to reconcile with the notion of delocalized radical ions. If the electron or hole in the AA excimer in a $(dA)_n$ sequence were delocalized, then this would probably affect the rate of charge recombination in the longer oligomers. However, if the average stacked domain is really only on the order of two bases in both $(dA)_2$ and $(dA)_{18}$, then radical ion delocalization may not be relevant to the experiments of Su et al. [9]. By the same token, the possibility that domains of three or more stacked bases are improbable would contradict the assumption by Bucher et al. [136] that the bases in their single strands are well stacked. It should also be noted that uracil has a low propensity for stacking [127, 170]. In any event, the very stimulating proposal that radical ions could be spatially delocalized in DNA invites further study.

5 Excited-State Dynamics in Base Pairs and in Double-Stranded DNA

The precise effects of base pairing on excited-state dynamics in nucleobase multimers are still uncertain and considerable effort is currently focused on this topic. Although the photophysics of base stacks can be studied in the absence of base pairing interactions using the dinucleotide and single-stranded model systems described in Sect. 4, study of base pairs in aqueous solution in the absence of base stacking is problematic. In water, bases will stack rather than form hydrogen bonds with one another, as demonstrated by self-association studies of base monomers [42, 43]. Consequently, a model system has not yet been found for preparing a single base pair in aqueous solution that is not simultaneously π-stacked with other bases as mentioned in Sect. 3.2.

The shortage of model systems for single base pairs in aqueous solution has not led to a shortage of hypotheses. One with a long history is the idea that UV excitation induces one or more protons in hydrogen bonds to move from one nucleobase to its base-paired partner [171]. Double proton transfer in two hydrogen bonds is illustrated for AT and GC base pairs in Fig. 11. By altering the tautomeric forms of the bases on both strands, UV-induced interstrand proton transfer (PT) would be mutagenic, if back PT to reform the starting bases were to be frustrated [171]. The lifetimes of $^1\pi\pi^*$ states of monomeric bases are virtually the

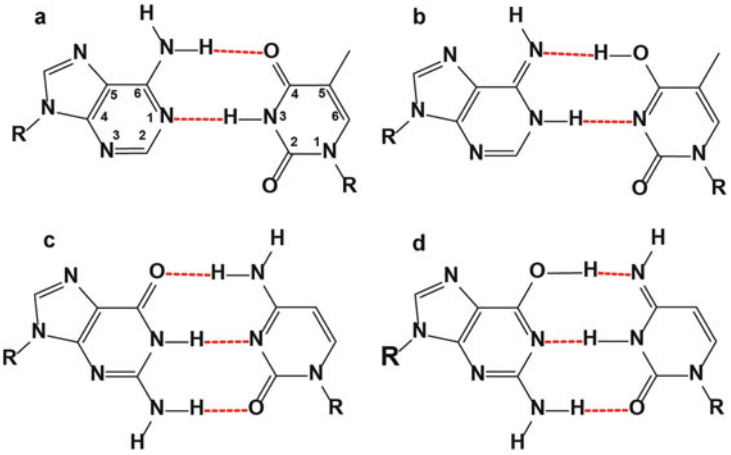

Fig. 11 A Watson–Crick AT base pair (**a**) before and (**b**) after double proton transfer (DPT). A Watson–Crick GC base pair (**c**) before and (**d**) after DPT

same in water and in aprotic solvents [172–174], indicating that deactivation does not involve excited-state proton transfer (ESPT). However, most of the canonical bases are stronger bases than water, and PT could be more favorable within a base pair than between a base and a solvent molecule.

The fundamental and as yet unanswered question is whether base pairing introduces new excited-state deactivation channels such as ESPT or the aborted hydrogen atom transfer mechanism suggested by Domcke and Sobolewski [175] (see below), or whether base pairing simply perturbs decay channels already operative in single bases and single strands. The latter possibility could reflect structural or steric constraints imposed by paired bases, or it could be a consequence of an altered dielectric environment caused by the exclusion of water molecules from the hydrogen bonding faces of the bases. This section reviews selected studies which address the above question. After discussing experiments on single base pairs in environments where they can be formed (i.e., in the gas phase and in low polarity solvents such as $CHCl_3$), results on double-stranded oligonucleotides made from stacked base pairs will be presented.

5.1 Single Base Pairs

A highly influential computational study by Sobolewski and Domcke considered excited state deactivation pathways in a single GC base pair [175]. This study introduced the stimulating proposal that aborted transfer of a hydrogen atom in a hydrogen bond joining the two bases mediates ultrafast decay to the electronic ground state. In particular, photoexcitation is proposed to populate a CT state in which an electron is transferred from G to C accompanied by motion of the N_1

proton along the middle of the three GC hydrogen bonds (the WC GC pair is illustrated in Fig. 11c). According to the calculations, proton transfer, driven by interstrand CT, leads to a CI with the ground state that is responsible for ultrafast deactivation. A similar paradigm was presented soon afterwards for a single AT base pair [176]. The Sobolewski and Domcke mechanism was invoked to explain the broad spectra observed for single WC GC base pairs in a supersonic jet using the IR-UV hole-burning technique by Abo-Riziq et al. [177]. Narrow spectra were observed for non-WC forms of the GC base pair, and the authors suggested that the special electronic structure of the WC pair leads to rapid excited-state quenching.

Although single base pairs will not form in aqueous solution, they can be prepared in nonpolar solvents, especially with suitably derivatized nucleobases. Schwalb and Temps [70] studied a modified GC base pair in chloroform using the fs-FU technique. They measured a fluorescence lifetime of 0.355 ps for the WC base pair, which is modestly shorter than the lifetimes of the separate G and C derivatives in the same solvent. Schwalb and Temps suggested that ultrafast PT in a GC base pair, perhaps taking place as suggested by Domcke and Sobolewski [175], could explain their observations.

More recent experiments on single base pairs in chloroform have revealed dynamics resembling those of a monomer and failed to document ultrafast PT [70, 178, 179]. TD-DFT calculations also indicate that even a weakly polar solvent can dramatically alter the energetics of the relevant excited states, leading to a barrier to PT not seen in the gas-phase calculations [178]. Significantly, long-lived excited states with lifetimes of ~20 ps are readily observed in a variety of duplexes formed from GC base pairs [180]. This is strong evidence that ultrafast excited-state decay is not the exclusive decay channel, or may not take place at all. Finally, a study of the planar A-A base pair in the gas phase by femtosecond time-resolved photoelectron spectroscopy showed only lifetimes resembling those of a monomer with no evidence of excimer states and no suggestion of PT [16].

5.2 Double-Stranded Oligonucleotides

A central message from Sect. 4 of this review is that excited-state delocalization in single strands depends strongly on whether or not the absorbing bases are present in stacked domains. In double strands, a high fraction of all bases are expected to be stacked compared to the more disordered single strands (see Sect. 3.3). The consequences of a greater degree of structural order on dynamics have been studied using both TA and time-resolved emission techniques [22, 118, 124, 181].

5.2.1 Long-Lived Excited States Are Observed in Stacked Base Pairs

An important generalization, first reported in 2005 [13], is that base pairing does not lead to strong quenching of the long-lived excited states seen in single-stranded

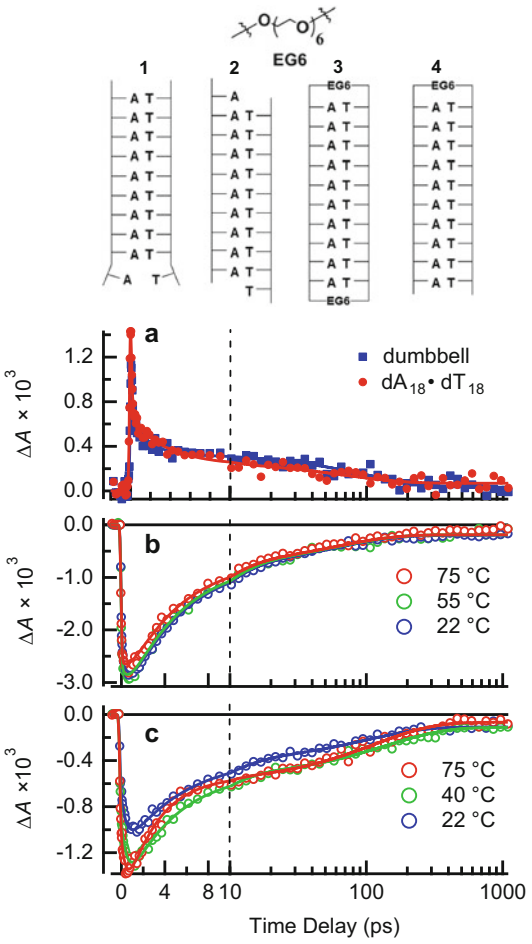

Fig. 12 *Top*: AT DNA homoduplexes with stacking and pairing defects (**1**, **2**) that are eliminated in the EG6-linked dumbbell (**3**) and hairpin (**4**) structures. fs-TA signals (pump 265 nm) (**a**) at room temperature from (3) and from duplex $dA_{18}{\cdot}dT_{18}$ at 350 nm, (**b**) from (3), and (**c**) from $dA_{18}{\cdot}dT_{18}$ at the indicated temperatures. The probe wavelength in panels b and c is 250 nm

nucleic acids. Crespo-Hernández et al. [13] reported that long-lived excited states in duplex $(dA)_{18} \cdot (dT)_{18}$ have similar decay kinetics compared with single-stranded $(dA)_{18}$, suggesting that AT base pairing neither inhibits the formation of, nor accelerates the decay of, excimers in the adenine strand.

Important new insights into the photophysics of double-stranded DNA were obtained from a study of DNA dumbbell and hairpin conjugates made up of AT base pairs (**3** and **4** in Fig. 12) [22]. The non-chromophoric hexa(ethylene glycol) linkers used in these AT conjugates increase the melting temperature by approximately 40°C compared to unlinked homo-duplexes with the same number of base pairs. These covalent linkers largely eliminate the slipped and frayed structures present in solution for low-melting $(dA)_n \cdot (dT)_n$ duplexes (**1** and **2** in Fig. 12), allowing the excited-state dynamics of stacked A · T base pairs to be observed without interference from structures with stacking or pairing defects.

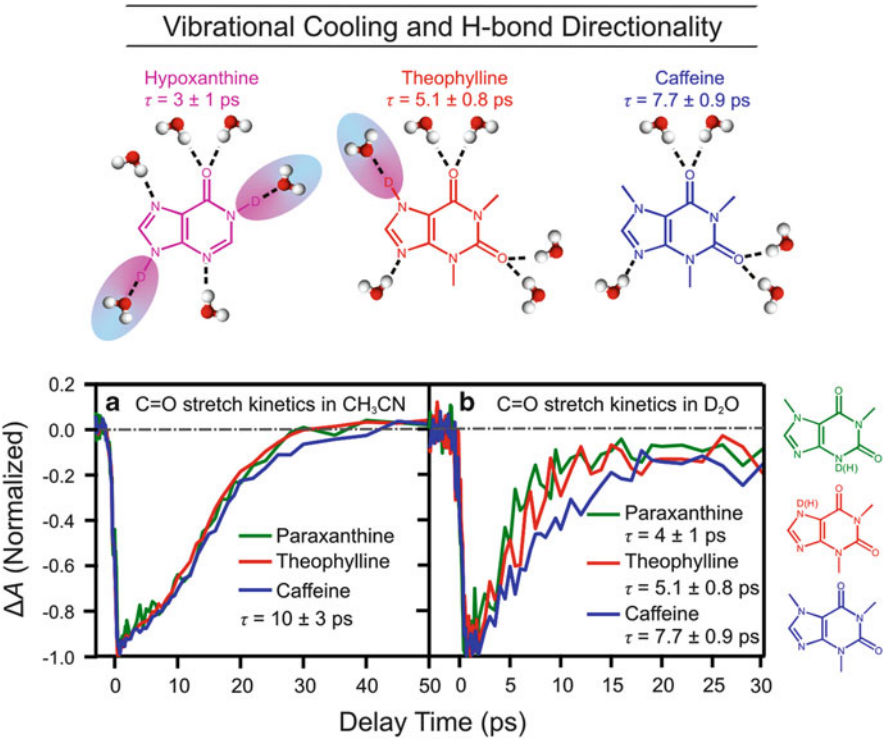

Fig. 13 *Top*: Vibrational cooling (VC) time constants in D_2O and H-bond donors; (*bottom*) bleach recovery kinetics for the carbonyl stretch ($\nu_{C=O}$) of several xanthines in (*a*) acetonitrile at 1,665 cm^{-1}, and (*b*) D_2O solution at 1,640 cm^{-1}. Figure adapted from [21]

UV pump/UV probe fs-TA signals for the dumbbell and hairpin structures decay on two widely separated time scales [22]. Results for the dumbbell are shown in Fig. 12b). A fast component of 4.7 ps is observed along with a slower component of ~70 ps. The fast component is assigned to VC following ultrafast IC – the latter process is seen in the subpicosecond decay of the excited-state absorption seen at 350 nm (Fig. 12a). The slow component of 4.7 ps is the slowest VC lifetime ever observed in double-stranded DNA made only of AT base pairs. For comparison, the VC lifetime of AMP is 2.3 ps [30]. A study [21] of VC by monomeric xanthine derivatives, which demonstrated a correlation between the count of solute hydrogen bond donor groups and VC rates (Fig. 13), provided the key to interpreting this surprising finding. In an AT base pair, two N-H bonds are formed with hydrogen bond acceptors on the complementary base, eliminating two hydrogen bonds with solvent molecules. Because the N–H modes are no longer in resonance with solvent OH stretches, VC occurs more slowly for structures with WC base pairs than for monomeric bases or single-stranded DNA.

Chen et al. recognized that the 70 ps lifetime measured for dumbbell **3** is substantially shorter than the lifetime reported in 2005 for the similar $(dA)_{18} \cdot (dT)_{18}$

duplex by Crespo-Hernández et al. [13]. A reinvestigation of the latter sample (see Fig. 12c) determined that the dynamics are in fact nearly identical to the dumbbell. Chen et al. concluded that the earlier results were obtained at an elevated temperature at which the duplex was substantially denatured [22]. The culprit was the spinning cell used in the 2005 study, which had a very small working volume. The slow (diffusion-limited) exchange between pumped and non-pumped volumes of the solution and the high efficiency of nonradiative decay by DNA resulted in a sample temperature of between 40°C and 50°C which denatured the low-melting AT homo-duplex discussed in the 2005 paper [13]. The use of a flow cell by Chen et al. in the 2013 study [22] completely eliminated laser-induced melting, and the authors were able to record accurately the excited-state dynamics of AT base pairs by the fs-TA technique for the first time (Fig. 12c).

The results in Fig. 12 establish that the long-lived excited states in both the dumbbell and in $(dA)_{18} \cdot (dT)_{18}$ decay somewhat more rapidly than excitations in single-stranded $(dA)_n$ sequences (70 vs 180 ps [9]). There is some quenching caused by base pairing, but this quenching occurs at a modest rate compared to the ultrafast deactivation predicted for GC base pairs [175]. The ~70-ps decay is essentially independent of temperature between 22°C and 75°C (Fig. 12b). This confirms that changes in excited-state dynamics seen in single-stranded and duplex DNAs without linkers at elevated temperatures are caused mainly by thermal disordering. On-going fs-TRIR experiments in Montana seek to understand the nature of this quenching.

A notable result from this study is the simultaneous presence in the fs-TA signals of a subpicosecond decay and the ~70 ps channel for the dumbbell. In the dumbbell, structural disorder is minimized and virtually all bases are stacked and paired. This is strong experimental evidence that ultrafast IC remains a significant decay channel in an A · T-DNA duplex system in which virtually all bases occur in stacked base pairs. The observation of fast and slow decay components in DNA single strands (Fig. 4) does not prove this because of the possibility that the fast component is caused by excitations localized on unstacked bases. Ultrafast IC in base stacks has been predicted theoretically [59, 108, 115, 182, 183].

The reduction in lifetime in the dumbbell (70 ps [22]) compared to dA_{18} (~180 ps [9]) is also not necessarily the result of modifications to electronic structure from base pairing. Recognizing that there are many stacking defects in single strands, one side effect of double strand formation is an increase in the average number of bases that are intimately stacked, and this could affect excimer-state dynamics. However, it would seem more reasonable to observe longer, and not shorter, lifetimes in longer stacks, if longer stacks facilitate escape by the radical ions formed by charge separation. It is possible that the fast decay channel seen in the dumbbell is caused after all by deactivation of at least some excited states by base pair-specific interactions. This observation pinpoints one of the current challenges to interpreting the biphasic dynamics seen in single- and double-stranded oligonucleotides: are the experiments observing the same decay channels in both systems or are the dynamics fortuitously similar even though fundamentally different excited states and decay channels are involved?

5.2.2 Long-Lived Excited States and Helix Conformation

AT base pairing measurably affects nonradiative decay rates in AT duplexes, but other experiments have shown that excimer lifetimes are insensitive to base-pairing motif and helix conformation [184]. de La Harpe et al. studied a $d(GC)_9 \cdot d(GC)_9$ duplex by fs-TA spectroscopy [184]. This self-complementary DNA duplex adopts different conformations in solution depending on the ionic strength and pH, allowing the effect of different base stacking motifs on excited-state dynamics to be studied in a system of constant base sequence.

In low salt conditions, $d(GC)_9 \cdot d(GC)_9$ adopts a typical B-form helix, but in high salt conditions the sequence undergoes a structural transition to the left-handed Z-form. Despite the starkly different base stacking geometries between the two conformations, nearly identical signals were observed for the B- and Z-conformations. The lifetime of the Z-form was measured to be 7.6 ± 0.8 ps at 250 nm probe in agreement with the 6.3 ± 0.6 ps lifetime measured for the B-form duplex within experimental uncertainty. TRIR experiments on poly(dGdC)·poly (dGdC) by Doorley et al. [185] revealed some differences in dynamics between B- and Z-form helices, but the authors commented that the relaxation occurs on similar time scales despite the considerable structural changes. Recently, GC hairpins with hexa(ethylene glycol) linkers were studied in TCSPC emission experiments by Brazard et al. [181]. The authors concluded that more ordered helices have measurable effects on the complex mix of emissive excited states.

A further result of interest with the alternating GC duplex follows from a comparison of fs-TA and TCSPC emission measurements. Bleach recovery signals measured in fs-TA experiments suggest that the vast majority of excitations (perhaps more than 95%) return to the electronic ground state in tens to hundreds of picoseconds when DNA strands are excited at UVB or UVC wavelengths. In contrast, sensitive TCSPC measurements have detected much longer-lived excited states which decay on the nanosecond time scale [121, 186]. Markovitsi et al. [124] estimated that 20% of excited states in alternating GC duplex polymers emit on the nanosecond time scale [124], yet GSB recovery signals measured for $d(GC)_9 \cdot d(GC)_9$ show that nearly all excited states decay within the first 100 ps after excitation [187]. Nanosecond emission components were also reported for $(dA)_{20}$ [121, 149]. Kwok and Phillips [23], who studied emission from the same substrate with lower time resolution, argued that any nanosecond time scale emission must be extremely weak. This is consistent with fs-TA GSB signals at both UV and mid-IR wavelengths, which show that excited states with nanosecond lifetimes in DNA single and double strands are formed in very low quantum yields under UVB/UVC excitation.

5.2.3 Proton-Coupled Electron Transfer in DNA

As discussed in Sect. 4, intrastrand CT or excimer/exciplex states are ubiquitous whenever bases are stacked in DNA. This suggests that charge separation along a strand could be coupled to proton transfer within a base pair (Fig. 14). This is a proton-coupled electron transfer (PCET) process initiated in DNA by UV radiation [187]. It differs from predicted PCET within a single base pair [175, 188] by proposing that 'vertical' ET (i.e., between stacked bases) triggers 'horizontal' PT (i.e., within a base pair). Calculations predict that barriers to PT are dramatically lower in singly oxidized and reduced base pairs [189–193].

Solvent kinetic isotope effects (KIEs) on the lifetimes of excited states have been observed in fs-TA experiments on double-stranded DNA model systems, especially in double strands with an alternating base sequence (e.g., GCGC...) in each strand [13, 187]. These experiments reveal coupling to proton coordinates but it is unclear whether the KIEs are a consequence of proton transfer or just represent a general solvent KIE on the rate of decay of an intrastrand CT state. For example, a pronounced solvent KIE is observed in fs-TA signals from $d(GC)_9.d(GC)_9$ in D_2O [187]. Compared with H_2O, the initial decay component remained the same, but a long-lived 22 ± 6 ps component with approximately half of the amplitude of the maximum ground-state bleach was observed in D_2O. Meanwhile, the same isotope effect was not observed in signals from the non-alternating d(C4G4)·d(C4G4) duplex.

A modified $d[(GX)_9GC]$ sequence, where X is 3-methylcytidine, was also studied by de La Harpe et al. [187]. The presence of the methyl group interferes with hydrogen bonding, causing this sequence to form a stacked single strand. The KIE observed in this case is very similar to the modest effect seen in an equimolar solution of C and G and is assigned to slower VC in D_2O vs H_2O for those excitations that decay via ultrafast IC to the electronic ground state. Thus, the absence of a strong KIE in the single-stranded $d[(GX)_9GC]$ sequence suggests that base pairing is responsible for the KIE seen in the $d(GC)_9.d(GC)_9$ double strand.

Computational studies have provided an additional perspective on PT in GC base pairs. Li et al. calculated that PT is energetically favorable for the GC radical anion base pair with a free-energy change of -3 kcal mol^{-1} [192]. Kumar and Sevilla found that proton transfer is favorable if water molecules are included to mimic the hydration environment in DNA. The free energy change was predicted to be -0.65 kcal mol^{-1} with an activation energy of 1.42 kcal mol^{-1} [195]. Ko and Hammes-Schiffer studied both intra- and interstrand CT states of model duplex structures with alternating and non-alternating GC base pairs [196]. The energy of the interstrand CT state decreases when the proton is displaced from G to C and a barrier may appear during this process. Meanwhile, the intrastrand CT states are less sensitive to proton displacement. These researchers also found that photoexcitation of the alternating duplex could lead to an intrastrand CT state, which could undergo a nonadiabatic transition to an interstrand CT state via proton transfer. Because of the relatively high energies of the intrastrand CT states, this pathway

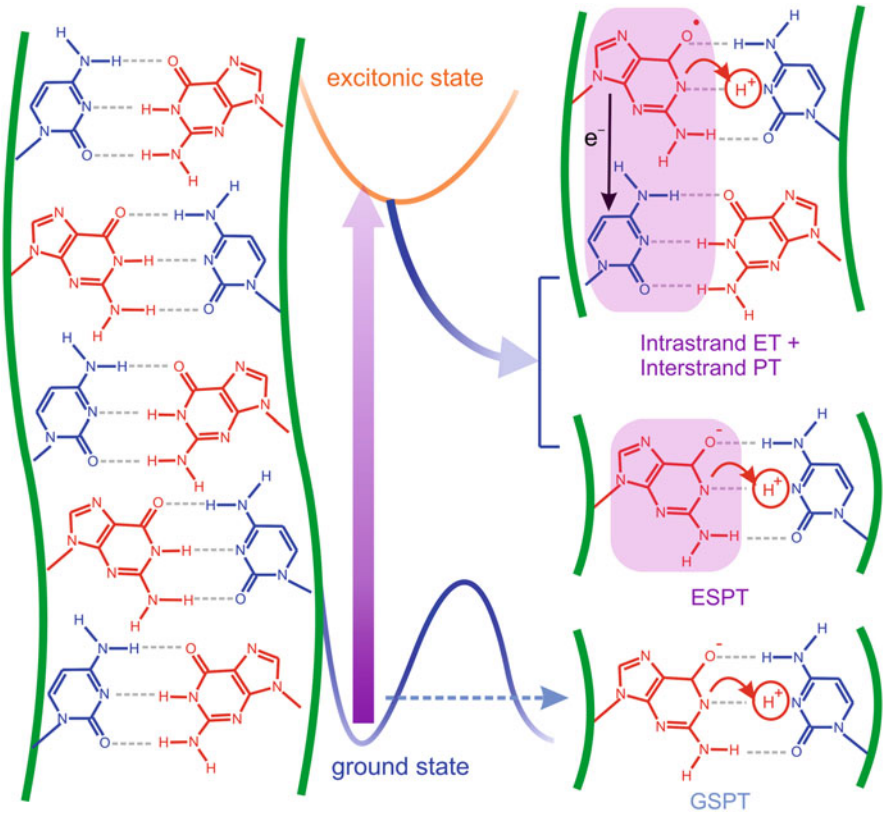

Fig. 14 Illustration of possible proton transfer and proton-coupled electron transfer events in an alternating GC duplex. GSPT: ground-state proton transfer. This single PT requires overcoming a calculated barrier of ~15 kcal mol^{-1} [191]. ESPT: excited-state proton transfer. Locally excited G transfers a proton to its base paired partner. The barrier to single PT is similar in the excited state as in the ground electronic state [194], but simultaneous transfer of an electron and a proton may be barrierless [175]. Intrastrand ET + Interstrand PT: photoexcitation transfers an electron from G to C on the same strand, followed by spontaneous interstrand PT from $G^{\bullet+}$ to C

was suggested to be isotopically sensitive and unavailable in the non-alternating sequences in support of the experimental results in [187].

6 Summary and Outlook

The reductionist approach to studying excited states in single and double strands of nucleic acids through carefully selected model systems has led to dramatic advances during the past decade. It is increasingly clear that interbase electron transfer is a major decay channel for excited states of DNA strands – a process that

requires π−π stacking of the bases. In stacked domains it has been shown that half or more of all excitations populate charge separated states that subsequently undergo charge recombination on time scales of tens to hundreds of picoseconds [136, 137]. Even the relatively long time constant of ~200 ps measured for the excimer lifetime in a dA-dA stack [9, 23, 27, 58, 132] appears to be faster than the time needed for the radical ions to diffuse away from one another or for photochemical reactions to take place.

Growing evidence that CT states are formed in DNA strands whenever bases are stacked has important consequences for understanding DNA photodamage. It will be important to determine whether nucleobase radical ion pairs produced by UV excitation can undergo subsequent chemical reactions prior to their recombination by back electron transfer. One possible outcome of photoinduced ET in DNA is repair of the cyclobutane pyrimidine dimer (CPD), the most ubiquitous photoproduct formed in DNA by UV light. There is keen interest in the possibility that UV light can repair a CPD by photoinduced ET from a more easily oxidized base [140, 197–199]. Nguyen and Burrows recently demonstrated that UV-B irradiation of 8-oxo-dGuo, a signature product of oxidatively damaged DNA, can repair CPDs in double-stranded DNA [138]. They attributed repair to ET from an excited electronic state of 8-oxo-dGuo to the CPD. The proposed pathway is reminiscent of how the flavin in photolyase repairs CPDs by photoinduced electron transfer [200, 201]. The ability of a damaged base to act in the same way as a repair enzyme has exciting implications for the early evolution of DNA.

Given the multiple classes of excited states created when DNA absorbs UV radiation – states populated either directly by absorption, or indirectly as intermediates along relaxation pathways back to the electronic ground state – an essential aim is to describe the lifetimes and yields of the various states. Understanding the nature of the emissive states with nanosecond lifetimes, which are formed in low yields (Sect. 5.2.2), and their relation to the much greater populations of excited states which decay on much faster time scales is an important future challenge. The proposal by Vayá et al. [186] that radical ions may occasionally escape to form free ions which contribute to the long-time emission merits study, especially because of the role that free ions could play in DNA photodamage.

The key structural motif that enables interbase electron transfer is base stacking, and experiments indicate that disrupting orbital-orbital overlap between stacked bases either by raising temperature or adding a denaturant completely eliminates this channel. These observations delineate important opportunities for electronic structure theorists to fill knowledge gaps surrounding fundamental nonradiative processes of electron and energy transfer in stacks of aromatic organic molecules. Adding base pairing interactions does not eliminate the CT states seen in single strands of stacked bases. It is an open question whether interstrand PT is an important deactivation mechanism for excited states in DNA [193, 202–205].

Nonetheless, differences are observed in double vs single strands such as slightly faster rates of decay and modest solvent kinetic isotope effects. These observations hint that intrastrand CT is coupled to proton coordinates. There have, however, been no direct observations to date of PT dynamics, either in the gas phase or in

solution, although this remains an important objective of on-going fs-TRIR experiments. Very recently, Hunger et al. [85] detected guanine radicals formed in H-bonded aggregates of guanine following UV excitation. However, PT was postulated to take place from a slowly formed triplet CT state, and the rate of PT was not determined [85]. There does not appear to be evidence from time-resolved spectroscopy that UV excitation induces proton transfer on a subnanosecond time scale in *any* DNA system. The notion that UV light initiates proton-coupled electron transfer in DNA also illuminates new frontiers for future experimental and theoretical investigation. *The gulf between theoretical predictions of PT in base pairs and the paucity of experimental evidence for this phenomenon* poses an engaging future challenge for experimentalists and theoreticians.

On the other hand, how these CT states, which do not appear to be directly populated by UV absorption, are reached from the initially populated excited states is uncertain, but evidence suggests that they are formed on an ultrafast time scale which is faster than the typical instrument response time of fs-TA and fs-FU instrumentation. Furthermore, recent evidence indicates that the efficiency of reaching the CT state is wavelength dependent: UVC excitation populates the CT state in higher yield than does UVB. This striking observation may provide valuable information on how the CT state is reached from an initial exciton.

The observation of length-independent excited-state dynamics for single-stranded A tracts, combined with the rapid and efficient formation of the CT state in minimal stacks with only two nucleobases, indicates that the excitation energy provided by the UV photon is delocalized over no more than two residues. This short delocalization length is a direct result of the marginally stable DNA single strands, where stacked bases are randomly distributed along the stack and are usually flanked by unstacked bases. Understanding the behavior of excitations in longer stacked domains such as those in duplex DNAs is an important future challenge.

As the nature of the states formed by UV excitation of DNA comes into sharper focus, more work is needed to understand how the non-covalent interactions found in DNA (base stacking and base pairing) control the dynamics of these states. Because these same motifs occur in other supramolecular architectures, efforts to understand photophysical decay channels in DNA can deliver fundamental insights applicable to understanding electron and energy transfer in diverse structures formed from organic building blocks. Future work targeting improved understanding of the feedbacks between electronic structure and conformational dynamics will play a central role. These challenging topics have been studied separately for many years, but spectroscopic and computational advances in the field of DNA photophysics, many of which are described in this volume, are now in place to explore fruitfully their overlap. Full understanding of the nature of excited states and their deactivation pathways will enable time-resolved spectroscopy to be an increasingly precise probe of conformational dynamics in nucleic acid molecules, eventually providing an experimental check on the molecular dynamics simulations used to predict structural dynamics on nanosecond and faster time scales [206].

Acknowledgments This work has been supported by grants from the Chemical Structure, Dynamics and Mechanisms Program of the National Science Foundation and from the NASA Astrobiology Program. Many current and former students, postdoctoral researchers, and collaborators have contributed to this work over the past 15 years. Their efforts, which are documented in the papers cited in this chapter, have been indispensible to the success of this work.

References

1. Kohler B (2010) J Phys Chem Lett 1:2047
2. Gustavsson T, Improta R, Markovitsi D (2010) J Phys Chem Lett 1:2025
3. Crespo-Hernández CE, Cohen B, Hare PM, Kohler B (2004) Chem Rev 104:1977
4. Middleton CT, de La Harpe K, Su C, Law YK, Crespo-Hernández CE, Kohler B (2009) Annu Rev Phys Chem 60:217
5. Kleinermanns K, Nachtigallova D, de Vries MS (2013) Int Rev Phys Chem 32:308
6. Takaya T, Su C, de La Harpe K, Crespo-Hernández CE, Kohler B (2008) Proc Natl Acad Sci USA 105:10285
7. Schreier WJ, Schrader TE, Koller FO, Gilch P, Crespo-Hernández CE, Swaminathan VN, Carell T, Zinth W, Kohler B (2007) Science 315:625
8. Schreier WJ, Kubon J, Regner N, Haiser K, Schrader TE, Zinth W, Clivio P, Gilch P (2009) J Am Chem Soc 131:5038
9. Su C, Middleton CT, Kohler B (2012) J Phys Chem B 116:10266
10. Ward DC, Reich E, Stryer L (1969) J Biol Chem 244:1228
11. Rist MJ, Marino JP (2002) Curr Org Chem 6:775
12. Thompson KC, Miyake N (2005) J Phys Chem B 109:6012
13. Crespo-Hernández CE, Cohen B, Kohler B (2005) Nature 436:1141
14. Kang H, Lee KT, Jung B, Ko YJ, Kim SK (2002) J Am Chem Soc 124:12958
15. Ullrich S, Schultz T, Zgierski MZ, Stolow A (2004) J Am Chem Soc 126:2262
16. Smith VR, Samoylova E, Ritze HH, Radloff W, Schultz T (2010) Phys Chem Chem Phys 12:9632
17. Banyasz A, Vayá I, Changenet-Barret P, Gustavsson T, Douki T, Markovitsi D (2011) J Am Chem Soc 133:5163
18. Towrie M, Grills DC, Dyer J, Weinstein JA, Matousek P, Barton R, Bailey PD, Subramaniam N, Kwok WM, Ma CS, Phillips D, Parker AW, George MW (2003) Appl Spectrosc 57:367
19. Towrie M, Doorley GW, George MW, Parker AW, Quinn SJ, Kelly JM (2009) Analyst 134:1265
20. Oliver TAA, Zhang Y, Ashfold MNR, Bradforth SE (2011) Faraday Discuss 150:439
21. Zhang Y, Chen J, Kohler B (2013) J Phys Chem A 117:6771
22. Chen J, Thazhathveetil AK, Lewis FD, Kohler B (2013) J Am Chem Soc 135:10290
23. Kwok W-M, Ma C, Phillips DL (2006) J Am Chem Soc 128:11894
24. Karunakaran V, Kleinermanns K, Improta R, Kovalenko SA (2009) J Am Chem Soc 131:5839
25. Pecourt J-ML, Peon J, Kohler B (2000) J Am Chem Soc 122:9348
26. Pecourt J-ML, Peon J, Kohler B (2001) J Am Chem Soc 123:10370
27. Crespo-Hernández CE, Kohler B (2004) J Phys Chem B 108:11182
28. Jou F-Y, Freeman GR (1979) J Phys Chem 83:2383
29. Hare PM, Crespo-Hernández CE, Kohler B (2007) Proc Natl Acad Sci U S A 104:435
30. Middleton CT, Cohen B, Kohler B (2007) J Phys Chem A 111:10460
31. Elles CG, Rivera CA, Zhang Y, Pieniazek PA, Bradforth SE (2009) J Chem Phys 130:13
32. Kovalenko SA, Dobryakov AL, Ruthmann J, Ernsting NP (1999) Phys Rev A 59:2369

33. Jailaubekov AE, Bradforth SE (2005) Appl Phys Lett 87
34. Tauber MJ, Mathies RA, Chen XY, Bradforth SE (2003) Rev Sci Instrum 74:4958
35. Zhang Y, Improta R, Kohler B (2014) Phys Chem Chem Phys 16:1487
36. Gustavsson T, Sharonov A, Markovitsi D (2002) Chem Phys Lett 351:195
37. Peon J, Zewail AH (2001) Chem Phys Lett 348:255
38. Gustavsson T, Sharonov A, Onidas D, Markovitsi D (2002) Chem Phys Lett 356:49
39. Pancur T, Schwalb NK, Renth F, Temps F (2005) Chem Phys 313:199
40. Markovitsi D, Gustavsson T, Talbot F (2007) Photochem Photobiol Sci 6:717
41. Markovitsi D, Onidas D, Talbot F, Marguet S, Gustavsson T, Lazzarotto E (2006) J Photochem Photobiol. A 183:1
42. Schweizer MP, Broom AD, Ts'o POP, Hollis DP (1968) J Am Chem Soc 90:1042
43. Broom AD, Schweizer MP, Ts'o POP (1967) J Am Chem Soc 89:3612
44. Valdes-Aguilera O, Neckers DC (1989) Acc Chem Res 22:171
45. Bloomfield VA, Crothers DM, Tinoco I Jr (1974) Physical chemistry of nucleic acids. Harper & Row, New York
46. Gray DM, Ratliff RL, Vaughan MR (1992) Methods Enzymol 211:389
47. Woody RW (1995) Biochem Spectroscopy 246:34
48. Berova N, Di Bari L, Pescitelli G (2007) Chem Soc Rev 36:914
49. Kypr J, Kejnovska I, Renciuk D, Vorlickova M (2009) Nucleic Acids Res 37:1713
50. Ke C, Humeniuk M, S-Gracz H, Marszalek PE (2007) Phys Rev Lett 99:018302
51. Seol Y, Skinner GM, Visscher K, Buhot A, Halperin A (2007) Phys Rev Lett 98:158103
52. Hatters DM, Wilson L, Atcliffe BW, Mulhern TD, Guzzo-Pernell N, Howlett GJ (2001) Biophys J 81:371
53. Mills JB, Vacano E, Hagerman PJ (1999) J Mol Biol 285:245
54. Banáš P, Mládek A, Otyepka M, Zgarbová M, Jurečka P, Svozil D, Lankaš F, Šponer J (2012) J Chem Theory Comput 8:2448
55. Chen AA, García AE (2013) Proc Natl Acad Sci U S A 110:16820
56. Olson WK, Bansal M, Burley SK, Dickerson RE, Gerstein M, Harvey SC, Heinemann U, Lu X-J, Neidle S, Shakked Z, Sklenar H, Suzuki M, Tung C-S, Westhof E, Wolberger C, Berman HM (2001) J Mol Biol 313:229
57. Rose IA, Hanson KR, Wilkinson KD, Wimmer MJ (1980) Proc Natl Acad Sci U S A 77:2439
58. Chen J, Kohler B (2014) J Am Chem Soc 136:6362
59. Olaso-González G, Merchán M, Serrano-Andrés L (2009) J Am Chem Soc 131:4368
60. Hunter RS, van Mourik T (2012) J Comput Chem 33:2161
61. Florián J, Šponer J, Warshel A (1999) J Phys Chem B 103:884
62. Jafilan S, Klein L, Hyun C, Florián J (2012) J Phys Chem B 116:3613
63. Šponer J, Leszczyński J, Hobza P (1996) J Phys Chem 100:5590
64. Šponer J, Šponer JE, Mládek A, Jurečka P, Bánaš P, Otyepka M (2013) Biopolymers 99:978
65. Ts'o POP, Melvin IS, Olson AC (1963) J Am Chem Soc 85:1289
66. Ts'o POP, Chan SI (1964) J Am Chem Soc 86:4176
67. Eimer W, Dorfmuller T (1992) J Phys Chem 96:6790
68. Hamlin RM Jr, Lord RC, Rich A (1965) Science (Washington, DC, USA) 148:1734
69. Kyogoku Y, Lord RC, Rich A (1967) J Am Chem Soc 89:496
70. Schwalb NK, Temps F (2007) J Am Chem Soc 129:9272
71. Schwalb NK, Michalak T, Temps F (2009) J Phys Chem B 113:16365
72. Plützer C, Hunig I, Kleinermanns K (2003) Phys Chem Chem Phys 5:1158
73. Asami H, Yagi K, Ohba M, Urashima S, Saigusa H (2013) Chem Phys 419:84
74. Šponer J, Jurečka P, Marchan I, Luque FJ, Orozco M, Hobza P (2006) Chem Eur J 12:2854
75. Lowe MJ, Schellman JA (1972) J Mol Biol 65:91
76. Brahms J, Michelson AM, van Holde KE (1966) J Mol Biol 15:467
77. Powell JT, Richards EG, Gratzer WB (1972) Biopolymers 11:235
78. Olsthoorn CSM, Bostelaar LJ, De Rooij JFM, Van Boom JH, Altona C (1981) Eur J Biochem 115:309

79. Buhot A, Halperin A (2004) Phys Rev E 70:020902
80. Donohue J, Trueblood KN (1960) J Mol Biol 2:363
81. Cohen B, Larson MH, Kohler B (2008) Chem Phys 350:165
82. Schwalb NK, Temps F (2009) J Photochem Photobiol. A 208:164
83. Miannay FA, Banyasz A, Gustavsson T, Markovitsi D (2009) J Phys Chem C 113:11760
84. Nguyen Thuan D, Haselsberger R, Michel-Beyerle M-E, Anh Tuan P (2013) ChemPhysChem 14:2667
85. Hunger K, Buschhaus L, Biemann L, Braun M, Kovalenko S, Improta R, Kleinermanns K (2013) Chem Eur J 19:5425
86. Changenet-Barret P, Hua Y, Markovitsi D (2014) Electronic excitations in guanine quadruplexes. Springer, Berlin Heidelberg, p 1
87. Schwalb NK, Temps F (2008) Science 322:243
88. Brahms J, Mommaerts WFH (1964) J Mol Biol 10:73
89. Cassani GR, Bollum FJ (1969) Biochemistry 8:3928
90. Ke CH, Loksztejn A, Jiang Y, Kim M, Humeniuk M, Rabbi M, Marszalek PE (2009) Biophys J 96:2918
91. Applequist J, Damle V (1966) J Am Chem Soc 88:3895
92. Luzzati V, Mathis A, Masson F, Witz J (1964) J Mol Biol 10:28
93. Nonin S, Leroy J-L, Gueron M (1995) Biochemistry 34:10652
94. Davis JT (2004) Angew Chem Int Ed 43:668
95. Gehring K, Leroy JL, Guéron M (1993) Nature 363:561
96. Leroy JL, Gueron M, Mergny JL, Helene C (1994) Nucleic Acids Res 22:1600
97. Holm AIS, Kohler B, Hoffmann SV, Nielsen SB (2010) Biopolymers 93:429
98. Plasser F, Lischka H (2012) J Chem Theory Comput 8:2777
99. Blancafort L, Voityuk AA (2014) J Chem Phys 140:8
100. Kasha M (1963) Radiat Res 20:55
101. Bouvier B, Gustavsson T, Markovitsi D, Millié P (2002) Chem Phys 275:75
102. Czader A, Bittner ER (2008) J Chem Phys 128:035101
103. Scholes GD, Ghiggino KP (1994) J Phys Chem 98:4580
104. Gould IR, Young RH, Mueller LJ, Albrecht AC, Farid S (1994) J Am Chem Soc 116:8188
105. Wang YS, Haze O, Dinnocenzo JP, Farid S, Farid RS, Gould IR (2007) J Org Chem 72:6970
106. Wang YS, Haze O, Dinnocenzo JP, Farid S, Farid RS, Gould IR (2008) J Phys Chem A 112:13088
107. Spata VA, Matsika S (2013) J Phys Chem A 117:8718
108. Improta R, Barone V (2011) Angew Chem Int Ed 50:12016
109. Voityuk AA (2013) Photochem Photobiol Sci 12:1303
110. Bouvier B, Dognon J-P, Lavery R, Markovitsi D, Millié P, Onidas D, Zakrzewska K (2003) J Phys Chem B 107:13512
111. Emanuele E, Markovitsi D, Millie P, Zakrzewska K (2005) ChemPhysChem 6:1387
112. Plasser F, Aquino AJA, Hase WL, Lischka H (2012) J Phys Chem A 116:11151
113. Mouret S, Philippe C, Gracia-Chantegrel J, Banyasz A, Karpati S, Markovitsi D, Douki T (2010) Org Biomol Chem 8:1706
114. Ritze HH, Hobza P, Nachtigallova D (2007) Phys Chem Chem Phys 9:1672
115. Santoro F, Barone V, Improta R (2009) J Am Chem Soc 131:15232
116. Conti I, Altoè P, Stenta M, Garavelli M, Orlandi G (2010) Phys Chem Chem Phys 12:5016
117. Santoro F, Barone V, Lami A, Improta R (2010) Phys Chem Chem Phys 12:4934
118. de La Harpe K, Kohler B (2011) J Phys Chem Lett 2:133
119. Zeleny T, Ruckenbauer M, Aquino AJA, Muller T, Lankas F, Drsata T, Hase WL, Nachtigallova D, Lischka H (2012) J Am Chem Soc 134:13662
120. Plasser F, Lischka H (2013) Photochem Photobiol Sci 12:1440
121. Banyasz A, Gustavsson T, Onidas D, Changenet-Barret P, Markovitsi D, Improta R (2013) Chem Eur J 19:3762
122. Stuhldreier MC, Temps F (2013) Faraday Discuss 163:173

123. Doorley GW, Wojdyla M, Watson GW, Towrie M, Parker AW, Kelly JM, Quinn SJ (2013) J Phys Chem Lett 4:2739
124. Markovitsi D, Gustavsson T, Vaya I (2010) J Phys Chem Lett 1:3271
125. Holcomb DN, Tinoco I Jr (1965) Biopolymers 3:121
126. Eisenberg H, Felsenfeld G (1967) J Mol Biol 30:17
127. Warshaw MM, Tinoco I Jr (1965) J Mol Biol 13:54
128. Ogasawara N, Inoue Y (1976) J Am Chem Soc 98:7048
129. Dolinnaya NG, Fresco JR (1992) Proc Natl Acad Sci USA 89:9242
130. Stuhldreier MC, Schüler C, Kleber J, Temps F (2011) In: Chergui M, Jonas D, Riedle E, Schoenlein R, Taylor A (eds) Ultrafast phenomena XVII proceedings of the 17th international conference, Snowmass, Colorado, USA, July 18–23, 2010 Oxford University Press, New York, p 553
131. Eisinger J, Guéron M, Shulman RG, Yamane T (1966) Proc Natl Acad Sci U S A 55:1015
132. Buchvarov I, Wang Q, Raytchev M, Trifonov A, Fiebig T (2007) Proc Natl Acad Sci U S A 104:4794
133. Lu Y, Lan ZG, Thiel W (2011) Angew Chem Int Ed 50:6864
134. Lu Y, Lan ZG, Thiel W (2012) J Comput Chem 33:1225
135. Onidas D, Gustavsson T, Lazzarotto E, Markovitsi D (2007) J Phys Chem B 111:9644
136. Bucher DB, Pilles BM, Carell T, Zinth W (2014) Proc Natl Acad Sci U S A 111:4369
137. Zhang Y, Dood J, Beckstead AA, Li X-B, Nguyen KV, Burrows CJ, Improta R, Kohler B (2014) Proc Natl Acad Sci U S A 111:11612
138. Nguyen KV, Burrows CJ (2011) J Am Chem Soc 133:14586
139. Zhang Y, Dood J, Beckstead A, Chen J, Li X-B, Burrows CJ, Lu Z, Matsika S, Kohler B (2013) J Phys Chem A 117:12851
140. Pan ZZ, Chen JQ, Schreier WJ, Kohler B, Lewis FD (2012) J Phys Chem B 116:698
141. Onidas D, Markovitsi D, Marguet S, Sharonov A, Gustavsson T (2002) J Phys Chem B 106:11367
142. Improta R, Santoro F, Barone V, Lami A (2009) J Phys Chem A 113:15346
143. Santoro F, Improta R, Avila F, Segado M, Lami A (2013) Photochem Photobiol Sci 12:1527
144. Dreuw A, Weisman JL, Head-Gordon M (2003) J Chem Phys 119:2943
145. Lange AW, Rohrdanz MA, Herbert JM (2008) J Phys Chem B 112:6304
146. Improta R (2008) Phys Chem Chem Phys 10:2656
147. Lange AW, Herbert JM (2009) J Am Chem Soc 131:3913
148. Szalay PG, Watson T, Perera A, Lotrich V, Bartlett RJ (2013) J Phys Chem A 117:3149
149. Markovitsi D, Talbot F, Gustavsson T, Onidas D, Lazzarotto E, Marguet S (2006) Nature 441:E7
150. Jimenez R, Fleming GR, Kumar PV, Maroncelli M (1994) Nature 369:471
151. Andreatta D, Lustres JLP, Kovalenko SA, Ernsting NP, Murphy CJ, Coleman RS, Berg MA (2005) J Am Chem Soc 127:7270
152. Furse KE, Corcelli SA (2010) J Phys Chem Lett 1:1813
153. Tazawa S, Tazawa I, Tso POP, Alderfer JL (1972) Biochemistry 11:3544
154. Guckian KM, Schweitzer BA, Ren RXF, Sheils CJ, Tahmassebi DC, Kool ET (2000) J Am Chem Soc 122:2213
155. Johnson WC Jr, Itzkowitz MS, Tinoco I Jr (1972) Biopolymers 11:225
156. Šponer J, Riley KE, Hobza P (2008) Phys Chem Chem Phys 10:2595
157. Norberg J, Nilsson L (1998) Biophys J 74:394
158. Murata K, Sugita Y, Okamoto Y (2004) Chem Phys Lett 385:1
159. Davis RC, Tinoco I Jr (1968) Biopolymers 6:223
160. Scott JF, Zamecnik PC (1969) Proc Natl Acad Sci U S A 64:1308
161. Stern N, Major DT, Gottlieb HE, Weizman D, Fischer B (2010) Org Biomol Chem 8:4637
162. Moser CC, Keske JM, Warncke K, Farid RS, Dutton PL (1992) Nature 355:796
163. Zhang WY, Yuan SA, Wang ZJ, Qi ZM, Zhao JS, Dou YS, Lo GV (2011) Chem Phys Lett 506:303

164. Dou YS, Liu ZC, Yuan S, Zhang WY, Tang H, Zhao JS, Fang WH, Lo GV (2013) Int J Biol Macromol 52:358
165. Markovitsi D, Onidas D, Gustavsson T, Talbot F, Lazzarotto E (2005) J Am Chem Soc 127:17130
166. Wilson RW, Callis PR (1976) J Phys Chem 80:2280
167. Nielsen LM, Hoffmann SV, Nielsen SB (2013) Photochem Photobiol Sci 12:1273
168. Tonzani S, Schatz GC (2008) J Am Chem Soc 130:7607
169. Shao F, Augustyn K, Barton JK (2005) J Am Chem Soc 127:17445
170. Simpkins H, Richards EG (1967) J Mol Biol 29:349
171. Löwdin PO (1963) Rev Mod Phys 35:724
172. Cohen B, Hare PM, Kohler B (2003) J Am Chem Soc 125:13594
173. Gustavsson T, Sarkar N, Lazzarotto E, Markovitsi D, Improta R (2006) Chem Phys Lett 429:551
174. Gustavsson T, Banyasz A, Sarkar N, Markovitsi D, Improta R (2008) Chem Phys 350:186
175. Sobolewski AL, Domcke W (2004) Phys Chem Chem Phys 6:2763
176. Perun S, Sobolewski AL, Domcke W (2006) J Phys Chem A 110:9031
177. Abo-Riziq A, Grace L, Nir E, Kabelac M, Hobza P, de Vries MS (2005) Proc Natl Acad Sci U S A 102:20
178. Biemann L, Kovalenko SA, Kleinermanns K, Mahrwald R, Markert M, Improta R (2011) J Am Chem Soc 133:19664
179. Roettger K, Soennichsen FD, Temps F (2013) Photochem Photobiol Sci 12:1466
180. Crespo-Hernández CE, de La Harpe K, Kohler B (2008) J Am Chem Soc 130:10844
181. Brazard J, Thazhathveetil AK, Vaya I, Lewis FD, Gustavsson T, Markovitsi D (2013) Photochem Photobiol Sci 12:1453
182. Santoro F, Barone V, Improta R (2007) Proc Natl Acad Sci U S A 104:9931
183. Improta R (2012) J Phys Chem B 116:14261
184. de La Harpe K, Crespo-Hernández CE, Kohler B (2009) ChemPhysChem 10:1421
185. Doorley GW, McGovern DA, George MW, Towrie M, Parker AW, Kelly JM, Quinn SJ (2009) Angew Chem Int Ed 48:123
186. Vayá I, Gustavsson T, Miannay FA, Douki T, Markovitsi D (2010) J Am Chem Soc 132:11834
187. de La Harpe K, Crespo-Hernández CE, Kohler B (2009) J Am Chem Soc 131:17557
188. Kumar A, Sevilla MD (2013) Photochem Photobiol Sci 12:1328
189. Colson AO, Besler B, Sevilla MD (1992) J Phys Chem 96:9787
190. Colson A-O, Besler B, Close DM, Sevilla MD (1992) J Phys Chem 96:661
191. Bertran J, Oliva A, Rodríguez-Santiago L, Sodupe M (1998) J Am Chem Soc 120:8159
192. Li X, Cai Z, Sevilla MD (2001) J Phys Chem B 105:10115
193. Kumar A, Sevilla MD (2010) Chem Rev 110:7002
194. Guallar V, Douhal A, Moreno M, Lluch JM (1999) J Phys Chem A 103:6251
195. Kumar A, Sevilla MD (2009) J Phys Chem B 113:11359
196. Ko C, Hammes-Schiffer S (2013) J Phys Chem Lett 4:2540
197. Chinnapen DJF, Sen D (2004) Proc Natl Acad Sci U S A 101:65
198. Holman MR, Ito T, Rokita SE (2007) J Am Chem Soc 129:6
199. Law YK, Forties RA, Liu X, Poirier MG, Kohler B (2013) Photochem Photobiol Sci 12:1431
200. Kao YT, Saxena C, Wang LJ, Sancar A, Zhong DP (2005) Proc Natl Acad Sci U S A 102:16128
201. Jorns MS (1987) J Am Chem Soc 109:3133
202. Shafirovich V, Dourandin A, Geacintov NE (2001) J Phys Chem B 105:8431
203. Shafirovich V, Dourandin A, Luneva NP, Geacintov NE (2000) J Phys Chem B 104:137
204. Shafirovich V, Dourandin A, Huang W, Luneva NP, Geacintov NE (1999) J Phys Chem B 103:10924
205. Shafirovich VY, Courtney SH, Ya N, Geacintov NE (1995) J Am Chem Soc 117:4920
206. Spoerlein S, Carstens H, Satzger H, Renner C, Behrendt R, Morader L, Tavan P, Zinth W, Wachtveitl J (2002) Proc Natl Acad Sci U S A 99:7998